1990

# The synthesis of ammonia from hydrogen and atomic nitrogen on the Rh(110) surface

Linda Gail Siemsen
*Iowa State University*

# INFORMATION TO USERS

The most advanced technology has been used to photograph and reproduce this manuscript from the microfilm master. UMI films the text directly from the original or copy submitted. Thus, some thesis and dissertation copies are in typewriter face, while others may be from any type of computer printer.

**The quality of this reproduction is dependent upon the quality of the copy submitted.** Broken or indistinct print, colored or poor quality illustrations and photographs, print bleedthrough, substandard margins, and improper alignment can adversely affect reproduction.

In the unlikely event that the author did not send UMI a complete manuscript and there are missing pages, these will be noted. Also, if unauthorized copyright material had to be removed, a note will indicate the deletion.

Oversize materials (e.g., maps, drawings, charts) are reproduced by sectioning the original, beginning at the upper left-hand corner and continuing from left to right in equal sections with small overlaps. Each original is also photographed in one exposure and is included in reduced form at the back of the book.

Photographs included in the original manuscript have been reproduced xerographically in this copy. Higher quality 6" x 9" black and white photographic prints are available for any photographs or illustrations appearing in this copy for an additional charge. Contact UMI directly to order.

U·M·I

University Microfilms International
A Bell & Howell Information Company
300 North Zeeb Road, Ann Arbor, MI 48106-1346 USA
313/761-4700 800/521-0600

Order Number 9035116

# The synthesis of ammonia from hydrogen and atomic nitrogen on the Rh(110) surface

Siemsen, Linda Gail, Ph.D.

Iowa State University, 1990

U·M·I
300 N. Zeeb Rd.
Ann Arbor, MI 48106

# The synthesis of ammonia from hydrogen and atomic nitrogen on the Rh(110) surface

by

**Linda Gail Siemsen**

A Dissertation Submitted to the

Graduate Faculty in Partial Fulfillment of the

Requirements for the Degree of

DOCTOR OF PHILOSOPHY

Department: Chemistry
Major: Physical Chemistry

Approved:

Signature was redacted for privacy.

In Charge of Major Work

Signature was redacted for privacy.

For the Major Department

Signature was redacted for privacy.

For the Graduate College

Iowa State University

Ames, Iowa

1990

## TABLE OF CONTENTS

# INTRODUCTION

A practical method for synthesizing ammonia from elemental nitrogen and hydrogen was discovered at the turn of the century at BASF in Germany. Over 2500 compositions for an ammonia catalyst were tried by Mittasch at BASF by 1914.[1] Most compositions included substances now recognized as catalyst poisons. The Fe-$Al_2O_3$-$K_2O$ catalyst was first introduced in 1914.[2] This catalyst has not fundamentally changed in the past 70 years. In 1988, the U. S. chemical industry produced 33 billion pounds of ammonia which was the fifth largest commodity chemical.[3] The yield is about 8-10 % ammonia at 500 degrees C per pass.[2] Because of the low yield, the ammonia is trapped and additional nitrogen and hydrogen are added before the nitrogen and hydrogen are recycled and passed over the active catalyst again. If thermodynamic constraints were limiting the yield, maximum conversion would be seen for high pressures and low temperatures.[1] The reaction to form ammonia requires the breaking of the N-N triple bond and H-H bonds. Hydrogen adsorbs dissociatively on iron.[1] Hydrogen bond breakage is facilitated by the surface. The Fe surface will also react with nitrogen to cause its dissociation but it is a relatively slow process compared with hydrogen dissociation.[4] The rate of ammonia formation is roughly equivalent to the rate of adsorption of nitrogen.[5] One of the difficulties in elucidating the mechanism for this reaction is that negligible amounts of ammonia are formed at low pressures for thermodynamic reasons. The techniques of surface science can only be operated at pressures below $10^{-4}$ torr whereas the catalytic reaction is run at 1 atmosphere or higher.

A continuing question is what adsorbed nitrogen species on the surface leads to

ammonia formation. The adsorbed species could be $N_2$(ads) or N(ads). The atomic nitrogen would react via an intermediate imine and amine. The $N_2$(ads) would proceed through a diimine and subsequently hydrazine to produce ammonia.[4] Various workers in the field have seen atomic N on transition metal surfaces as a result of the decomposition of ammonia.[4] A logical extension has been to produce that intermediate in a different way and see if it produces ammonia. By forming and adsorbing atomic nitrogen on the surface, two steps in the postulated mechanism are replaced with one. The adsorption of molecular nitrogen and its subsequent dissociation are replaced with the adsorption of atomic nitrogen. The 109 kcal/mole will no longer be needed to break the adsorbed N-N double bond.[6] Another advantage to atomic nitrogen as a starting material is that lower pressures as well as a transition metal which does not dissociate nitrogen will work for ammonia synthesis under these conditions.

The next question is how to form atomic nitrogen. There are numerous methods such as light induced dissociation, a hot filament, electron impact on nitrogen on the surface, and plasmas. A plasma is produced by accelerating randomly occurring free electrons by electromagnetic energy. These free electrons can ionize gas molecules which produce more electrons. The current rises and a steady state is soon reached. Plasmas are relatively inexpensive to create and also capable of forming large quantities of intermediates such as atomic nitrogen. There are four major types which vary in the form of electromagnetic energy used - direct current, alternating current, $R_f$, and microwave. A microwave plasma was chosen for this work since microwave plasmas are the best method to dissociate homonuclear diatomics. A fortuitous aspect of this work is that by adding hydrogen to the nitrogen flowing through the plasma the dissociation of nitrogen increases. Another advantage for the microwave plasma is that

the microwave cavity fits around the outside of the glass tubing, so the only metal surfaces inside the glass tubing are the catalyst and its electrical and mechanical connections. This is a clear advantage over experiments which synthesize ammonia with a direct current induced plasma. A direct current plasma requires electrodes which are usually made of tungsten. Tungsten also can dissociate nitrogen and catalyze ammonia synthesis so the reaction to form ammonia in these systems could occur without the atomic nitrogen, electronically excited molecular nitrogen, and other transients produced by the plasma.[4] The atomic nitrogen on the catalyst could have been dissociated by the plasma or the tungsten surface. Another advantage to this work is that the distance between the plasma and the catalyst is such that the shorter lived species have largely decayed by the time the gas reaches the catalyst, so that atomic nitrogen is the predominant "excited" species there. This was not the case with the direct current plasmas.

Further clarification in the mechanism is found by choosing rhodium as a catalyst. Nitrogen adsorbs associatively on rhodium.[7] Rhodium does not form ammonia in measurable amounts for ammonia synthesis from the elemental gases. This means that any ammonia produced on the rhodium is due to the species produced by the plasma. In summary, this thesis will show that hydrogen and atomic nitrogen produce ammonia on Rh(110) and that forming a reactive intermediate such as atomic nitrogen bypasses the need for high pressures and thereby leads to a route by which ammonia synthesis can be studied under UHV conditions.

# LITERATURE REVIEW

This review is intended to summarize those aspects of the literature which are the most pertinent to this thesis. The major components will be a brief general summary on ammonia synthesis and mechanisms, evidence for atomic nitrogen as an intermediate for ammonia synthesis, adsorption of nitrogen and decomposition of ammonia on rhodium, formation and reactions of active nitrogen and atomic nitrogen, and plasma results for ammonia synthesis. Ammonia synthesis, particularly on the industrial Fe-$Al_2O_3$-$K_2O$ catalyst, has been extensively studied to understand the mechanism and to learn how to increase the efficiency of the overall reaction. These studies included the chemisorption of hydrogen and nitrogen on industrial ammonia catalysts. Hydrogen is chemisorbed dissociatively on iron below 500° C.[8] The temperature used for the commercial synthesis is approximately 500° C so the dissociation of hydrogen is a facile step.[9] However, the chemisorption of nitrogen on iron is not facile at the synthesis temperatures. The energy of activation for nitrogen chemisorption varies from 10 to 30 kcal depending on the fractional coverage of adsorbed nitrogen.[10]

One of the first steps in elucidating the mechanism of ammonia synthesis was the discovery that the overall rate of nitrogen adsorption at low coverages is roughly equal to the rate of ammonia synthesis.[5] It is also known that hydrogenation occurs much faster than nitrogen adsorption. There are two major choices for ammonia synthesis.[4]

(1) Molecular

$$N_2(g) + 3H_2(g) \rightarrow N_2(ads) + 6H(ads)$$

$$N_2(ads) + 6H(ads) \rightarrow N_2H_2(ads) + 4H(ads)$$

$N_2H_2(ads) + 4H(ads) \rightarrow N_2H_4(ads) + 2H(ads)$

$N_2H_4(ads) + 2H(ads) \rightarrow 2\ NH_3(ads)$

$2\ NH_3(ads) \rightarrow 2\ NH_3(g)$

(2)Dissociative

$N_2(g) + 3\ H_2(g) \rightarrow 2\ N(ads) + 6\ H(ads)$

$2\ N(ads) + 6\ H(ads) \rightarrow 2\ NH(ads) + 4\ H(ads)$

$2\ NH(ads) + 4\ H(ads) \rightarrow 2\ NH_2(ads) + 2\ H(ads)$

$2\ NH_2(ads) + 2\ H(ads) \rightarrow 2\ NH_3(ads)$

$2\ NH_3(ads) \rightarrow 2\ NH_3(g)$

The dissociative adsorption of hydrogen on iron was already well known in the 1930s so this is assumed in both mechanisms. A persistent question is whether the nitride of iron is formed. $Fe_4N$ and $Fe_2N$ are known. $Fe_4N$ can be formed from ammonia at 500° C.[9] There is also evidence a c(2x2) overlayer formed on a Fe(100) surface is quite similar to the geometry of the (002) plane of $Fe_4N$.[11] Metals which form interstitial nitrides from Group IVB to VIII are active as ammonia synthesis catalysts.[9] Atomic nitrogen would be more likely to form a nitride with a metal than molecular nitrogen, so this is additional evidence for the dissociative mechanism. $NH_{ad}$, formed as a result of ammonia decomposition, has also been observed by secondary ion mass spectrometry.[11] There is also evidence for atomic nitrogen on iron surfaces. On doubly promoted industrial catalysts little or no molecular nitrogen is present around 400-450° C.[10] Rapid isotopic mixing of nitrogen is catalyzed by Fe at 500° C. This rate for mixing is comparable to the rate of nitrogen desorption on the same catalyst.[10] Yet another aspect of the industrial catalyst is the role of the

promoters, $K_2O$ and $Al_2O_3$. The catalyst contains 0.6- 2% $Al_2O_3$ and 0.3 - 1.5% $K_2O$.[9] The alumina is believed to prevent the sintering of catalyst particles.[8] $K_2O$ is thought to facilitate the dissociation of nitrogen[8], similar to metallic potassium.

The importance of the thermodynamics to the overall yield has already been discussed.

$$N_2(g) + 3\ H_2(g) \rightarrow 2\ NH_3(g)$$

$$\Delta H_{273} = -46\ kJ/mole^4$$

$$K_p = P_{NH_3}/ P_{N_2}{}^{0.5} P_{H_2}{}^{1.5} \approx Ae^{-\Delta H/RT}$$

The reaction is exothermic [$\Delta H<0$] so low temperatures favor the formation of ammonia at equilibrium. But at low temperatures the rate of reaction is unsatisfactorily slow. A major function of a catalyst in this reaction is to permit the synthesis to be carried out at a satisfactory rate at a temperature such that the equilibrium also provides an acceptable yield. High pressures also favor the formation of ammonia; for example in a stoichiometric mixture, $P_{H_2} = 3\ P_{N_2}$, at a total pressure of 600 torr at 720 K the equilibrium pressure of ammonia is only 1 torr.[4] Doubling the initial total pressure would approximately quadruple the ammonia pressure at equilibrium in this case.

Many other single metals show activity for ammonia catalysis. For synthesis, these include Co, Ni, Ru, Os, Mn, Mo, W, Re, Cr and V.[9] Under conditions of 500 ° C, 60 $lh^{-1}$ flow rate, and pressures of 100 atmospheres, the most reactive of these metals are iron and osmium which both produce a 2% yield of ammonia under these conditions. Only ammonia decomposition has been observed for Ta, Rh, Pt, Pd, Ir, and Cu under these conditions.[9]

The focus of the ultrahigh vacuum work has been on Fe single crystal to model

more closely the industrial process. A starting point for UHV investigations has been the chemisorption of nitrogen on a clean single crystal surface. Work by Bozso et al. has shown that the Fe(111) face has the highest adsorption rate followed by the Fe(100) and Fe(110) at 550 K; adsorption rates are in ratios 60:3:1, respectively.[12] Not only do the crystal faces of iron vary in their ability to chemisorb nitrogen, variation is also seen in the activity to produce ammonia. The Fe(111) face was the most active. The ratio of activity is 418:25:1 for Fe(111), Fe(100), and Fe(110). This work was done at 20 atm for $P_{H_2}/P_{N_2}$ ratios of 3:1.[13] Another aspect of the UHV work on Fe(111) is the role of K on the surface. The K serves to promote the dissociation of nitrogen which is consonant with the purpose of this work. A high resolution electron energy loss spectroscopy (HREELS) study by Whitman et al. shows that low amounts of potassium ($<1.4 \times 10^{14}$ $cm^{-2}$) are enough to dramatically enhance the sticking coefficient of a $\pi$ bonded nitrogen precursor to dissociation on Fe(111).[14] This precursor which was formed in the presence of potassium has a N-N stretching frequency less than 20 $cm^{-1}$ lower than that of nitrogen which is $\pi$ bonded to the surface without potassium present. This result is in disagreement with other work which suggests that the N - N bond is sufficiently weakened when the surface has been promoted with potassium to significantly facilitate its breakage.

Evidence for atomic nitrogen as an intermediate for ammonia synthesis without potassium present comes from HREELS work by Bassignana and coworkers.[15] Ammonia was adsorbed on Ni(110) at 110 K. $NH_2$ and NH were identified by their characteristic vibrations. $NH_2$ fragments into NH + H and N + 2 H at 430 K and NH fragments around 500 K. Beyond 550 K only atomic nitrogen is left at the surface and its presence was inferred from thermal desorption.

Further evidence that atomic N is an intermediate for ammonia synthesis was

found in reactions of NO and $H_2$ over Rh foil.[16] Nitric oxide adsorbs dissociatively on Rh as evidenced by the isotopic exchange of $^{14}N^{18}O$ with $^{15}N^{16}O$. Twenty percent of the nitric oxide was exchanged at 600 K. The onset of exchange was at 400 K. Small amounts of ammonia were formed at temperatures around 500 K but not at higher temperatures. Since nitric oxide adsorbs dissociatively on Rh, a similar question is whether $N_2$ dissociates on Rh or any of the other platinum group metals. Nitrogen will dissociate on a Pt filament on special active sites with an apparent sticking coefficient of approximately $10^{-4}$.[4,17] The amount of dissociation depended only on the time of exposure. For Pd, no dissociative adsorption is seen for nitrogen.[18] For the case of Ir, the bonding of nitrogen is molecular below 300 K in ultrahigh vacuum systems.[19]

Rhodium, iridium, and palladium are known to catalyze ammonia decomposition at high temperatures but have not been reported to catalyze ammonia synthesis.[9] Pt is known to catalyze ammonia synthesis at 900° C and is active for decomposition as well.[9] If Rh and Ir are promoted with potassium metal, they are effective as ammonia synthesis catalysts. The conditions were 200-460° C, 600 torr nitrogen and hydrogen in a 1:3 mixture respectively and 4.5 $lh^{-1}$ flow rate.[20] The rate of ammonia synthesis over 2.5 g of 5 weight % Rh and Ir supported on active carbon which were promoted with 15 mg of potassium resulted in rates comparable to K promoted Fe under these conditions. The K promoted Pd catalyst did not produce ammonia in detectable amounts. The potassium changes the surface conditions of the Rh and Ir such that the barrier for nitrogen dissociation is lowered.

Because of the principle of microscopic irreversibility, results for ammonia decomposition on rhodium are important. Thermal desorption results from ammonia

adsorption at 250 K have shown a hydrogen/nitrogen peak at 350 K which was attributed to the $Rh_2NH$ species.[21] A nitrogen peak was present at 600 K. The nitrogen peak is due to the recombination of atomic nitrogen on the surface. No ammonia desorption was observed. Rh(110) had the highest rate for ammonia decomposition of the three Rh faces studied which were Rh(111), Rh(110), and Rh(100). The temperatures studied were 580-725 K and pressures from 0.001 -.0250 torr ammonia, 0.001- 0.0150 torr hydrogen and 0.001 - 0.250 torr nitrogen. Atomic nitrogen was also seen in ammonia decomposition on Ni(110).[15] Nitrogen which had been activated by ion gauge and mass spectrometer filaments to form atomic nitrogen was adsorbed and subsequently desorbed as molecular nitrogen in a peak at 670 K. As previously mentioned, NO adsorbs dissociatively on rhodium; thus dosing poly-crystalline rhodium with NO also leads to N(ads) which on heating gives a nitrogen desorption peak at 650 K.[22]

A recent mechanism suggests that dissociation occurs in the $N_2$/Fe(111) system via a molecular precursor. This precursor is thought to correspond to an electronically excited state of nitrogen. XPS data for nitrogen adsorption and dissociation have shown on Fe(111) that a weakly bound $\gamma$ state is converted to a strongly bound $\alpha$ state and then subsequently to what the authors describe as atomic nitrogen.[23] HREELS spectra show two peaks for $^{15}N_2$ on Fe(111) at 110 K. One is at 435 $cm^{-1}$ and the other at 1490 $cm^{-1}$.[24] The molecular N-N stretch is ascribed to the higher energy loss peak and the 435 cm to the Fe-N stretch. As the temperature is raised or as time passes, the N-N stretch is reduced in intensity. This is attributed to the dissociation of the $\alpha_1$ state to atomic nitrogen. The $\alpha_1$ nitrogen state is assigned a side-on bonding geometry where both N atoms interact with iron atoms.

Angle resolved ultraviolet photoelectron spectroscopy (ARUPS) results have

shown a strongly adsorbed α phase for nitrogen on the Fe(111) surface.[25] The nitrogen bond axis is strongly inclined with respect to the surface normal. It has been suggested that the α-$N_2$ state is a stabilized $^3\Sigma_u^+$ state of nitrogen. The vibrational frequency for the $^3\Sigma_u^+$ state is very close to that of the α nitrogen state and the bond length is 0.2 angstroms longer than in the ground state. It is stabilized by 2 N-Fe single bonds.

Another piece of evidence for atomic nitrogen as an intermediate in ammonia synthesis is given by Matsushita and Hansen.[26] They were able to duplicate the types of adsorbed nitrogen (β + x), resulting from the decomposition of ammonia, and observed by flash desorption studies, by adsorbing pure nitrogen activated in the gas phase by electron impact on nitrogen gas. This can also be prepared by thermal activation. The x state was identified as atomic nitrogen. First order recombination of the atomic nitrogen on the glass wall was also observed. Preparation of atomic nitrogen is analogous to formation by a plasma.

The low pressure nitrogen afterglows which are formed by plasmas are chemically reactive. (An afterglow is the region after the plasma which often emits light due to the excited species formed in the plasma.) Lord Rayleigh was one of the first to investigate this phenomenon and to observe characteristic excited species emissions. More studies have led to the conclusion that the reactivity is from metastable nitrogen atoms and molecules that are present.[27] In this thesis, active nitrogen refers to all the species present in the afterglow of the plasma including atomic nitrogen. The species most likely to play a leading role in active nitrogen include $N(^2D)$, $N(^2P)$, $N(^4S)$, $N_2$ $^5\Sigma_g^+$, $N_2$ $^3\Delta_u$ and $N_2$ $A^3\Sigma_u^+$. The $N(^2D)$ and $N(^2P)$ states are found near the plasma. These excited state atoms as well as $N_2$ ($A^3\Sigma_u^+$) are destroyed within a few

milliseconds.[28,29] The degree of dissociation of nitrogen by the microwave discharge is much less than 5 percent and is very sensitive to impurities such as oxygen, nitric oxide, hydrogen and sulfur hexafluoride. The addition of impurities can increase the nitrogen atom concentration by a factor of twenty.[29] There are two major routes for the quenching of electronically excited nitrogen ($A^3\Sigma_u^+$) to ground state molecular nitrogen ($X^1\Sigma_g^+$). The first is with ground state nitrogen atoms ($^4S$) and the second is with ground state nitrogen molecules. The reaction with ground state N atoms is 6 orders of magnitude faster.[30] This reaction is postulated to produce N($^2P$) which decays quickly to N($^4S$).

Several examples are known for ammonia synthesis through the use of a plasma. These examples range in pressure from 5-100 torr, vary in the type of discharge and in the catalyst chosen. The first example consists of an alternating current glow discharge with internal aluminum electrodes which were connected to the outside by tungsten leads.[31] This produces active nitrogen. The pressure was 10 torr and the $N_2/H_2$ ratio was 2:1. The discharge current was 8 mA. The active nitrogen reacts with hydrogen to form ammonia in this setup. As was pointed out in the introduction, there are several possible routes for ammonia formation. The species present in active nitrogen can then react on tungsten or aluminum to form ammonia. When an iron mesh catalyst was placed in the plasma zone, the amount of ammonia produced increased. NH and $NH_2$ were present in the gas phase during this experiment and were observed in the plasma. The emission spectra were taken through a slit in the microwave cavity.

A second system for ammonia production from plasmas consists of a direct current glow discharge with tungsten or stainless steel electrodes. Several examples of ammonia production from active nitrogen with this type of setup are known. The first utilized a Pt gauze inside for the DC discharge at a pressure of 100 torr and 35 mA of

current.[32] A second method employed wires wrapped around the inner electrodes. The wires were Pt, Cu, Fe, Ni, and Pd.[33] A maximum rate was seen for a $H_2$:$N_2$ ratio of 3:2 for this catalytic setup. Pressure for this experiment ranged from 1- 2 torr. The order of activity was Pd >Pt > Fe > Cu > Ni. A third example is for ammonia synthesis on zeolites utilizing a microwave discharge. The frequency was 2450 MHz and the power was 200 watts. The optimum yield was obtained for a molar ratio of .75 moles hydrogen to total moles of nitrogen and hydrogen.[34,35]

The plasma work shows clearly that the excited species produced in the plasma react on the metal surfaces to form ammonia. There is also evidence that excited species are formed as a result of reactions on the surface. Two examples illustrate such evidence, the first involving CO oxidation on Pt and the second ammonia decomposition on Pt. In the first case, the internal energy distributions of $CO_2$ were measured with Fourier transform infrared emission spectroscopy.[36] An effective description of the internal energy distribution in the product $CO_2$ is provided by an apparent temperature for each internal energy mode. The internal energy mode temperatures are substantially higher than the surface temperature. The activated complex for this reaction was modelled by assuming the activated state and the final product have similar structures. The conclusion was that the transition state was a $CO_2$ molecule slightly bent with the C end down.

A result bearing more closely on work in this thesis was evidence for the formation of vibrationally excited molecules in the catalytic decomposition of ammonia on polycrystalline platinum.[37] This reaction was studied with a molecular beam mass spectrometer. A large fraction of the nitrogen molecules evolved in the reaction had ionization potentials lower than that of the ground state nitrogen. A significant number

had ionization potentials as low as 14.25 eV or 1.3 eV less than ground state $N_2$. This would require excitation to the v=5 level of nitrogen (1.409 eV). In conclusion these two papers illustrate how excited species adsorbed on surfaces may play important roles in surface chemistry. Clearly, ammonia can be formed from the active nitrogen which has been produced by a plasma in the presence of hydrogen. Just as clearly, a kinetic study which shows the effect of atomic nitrogen instead of active nitrogen and incorporates a well characterized surface such as a single crystal will be of interest. The following experiments will illustrate the role atomic nitrogen can play in the synthesis of ammonia.

# EXPERIMENTAL

In order to study the synthesis of ammonia from hydrogen and atomic nitrogen on platinum and rhodium, atomic nitrogen must be produced and characterized. Atomic nitrogen is for a reactive intermediate a relatively long-lived transient species. To produce such an intermediate in quantities sufficient for the purposes of this reaction requires a plasma. A microwave induced plasma was the best choice - for ease of use and reproducibility. The afterglow was characterized in two ways. The first method was by ultraviolet-visible emission spectroscopy. This revealed the presence of several species produced by the plasma and in addition showed that species resulting from the combination of N and H (for example NH and $NH_2$) were not detectable. However, the characteristic emission from the $^2P \rightarrow {}^4S$ transition for atomic nitrogen was not observed due to the weakness of this particular transition. This led to further characterization and quantitation by a gas phase titration, specific for atomic nitrogen, which will be discussed later. Once the atomic nitrogen was fully characterized, the focus of attention turned to the reaction of the atomic nitrogen. Did it react to produce ammonia and how did variations in the pressures of atomic nitrogen and hydrogen affect the rate of ammonia production? A kinetic system was designed to answer these questions.

## Kinetic System and Materials

An overview of the system design is shown in a flow chart (Figure 1). Nitrogen and hydrogen are introduced into the system using a mixer which had been calibrated

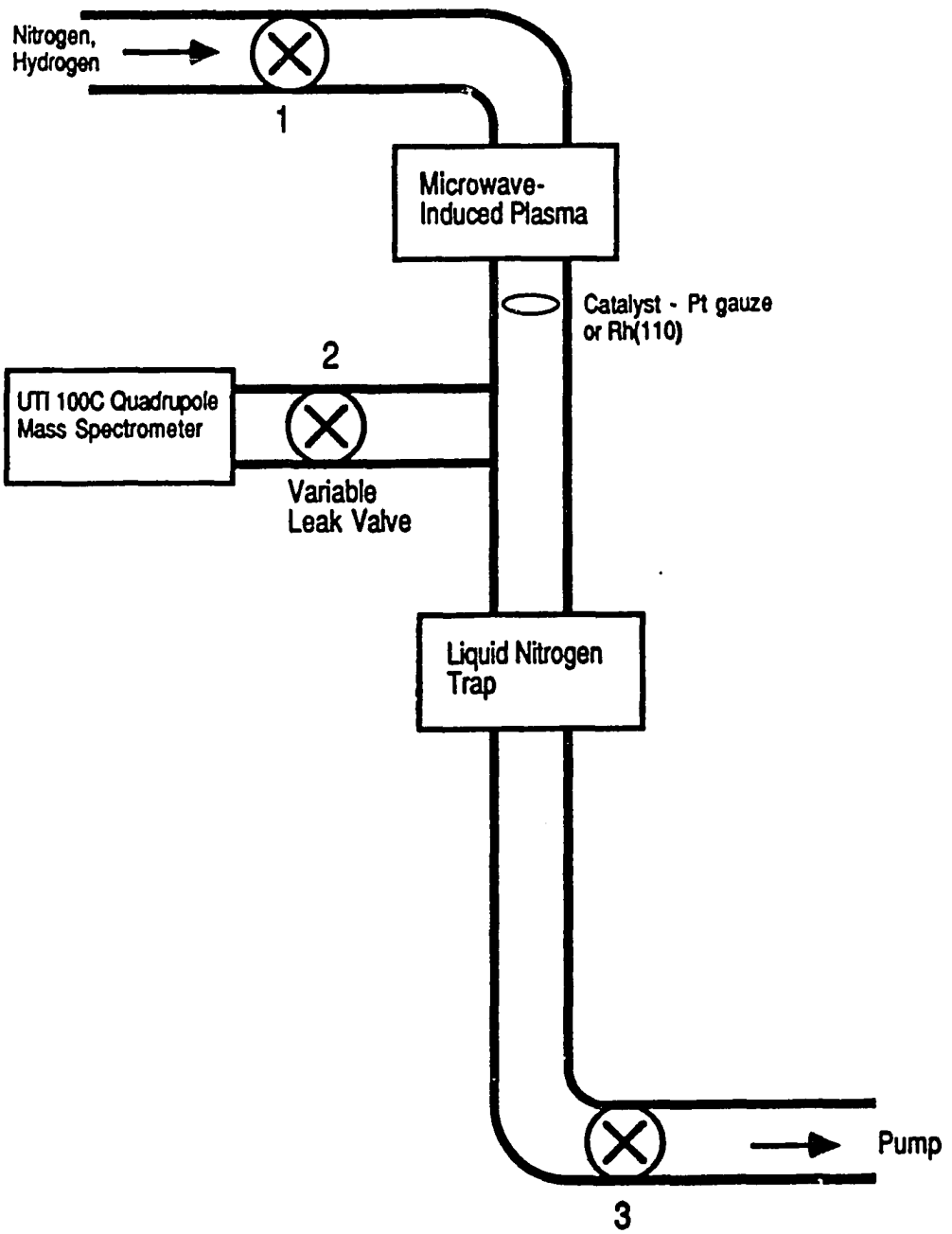


Figure 1. A schematic of the kinetic system

for the respective flow rates of these two gases. The gases then passed through the microwave cavity which coupled the gas to the microwave radiation supplied by the microwave power supply at 2450 MHz. The catalyst which was platinum gauze for the early experiments and subsequently Rh(110) was placed 33 mm downstream from the edge of the Evenson microwave cavity in the afterglow region. The ammonia which was produced on the catalyst was condensed in a liquid nitrogen trap. At the end of a run (typically two hours) the trap was warmed after valves 1 and 3 were closed. The variable leak valve was opened and the amounts of ammonia and other products were quantified by the mass spectrometer.

Nitrogen and hydrogen gas flows were measured and combined using a gas mixer (Matheson 7352) with 610 tube cubes. These tube cubes measured flow rates up to 200 ml/minute and the gases were combined in a mixing tube. The flow rates for both the nitrogen and hydrogen were controlled by high accuracy needle valves. Typical flow rates ranged from 0.5 ml/minute < nitrogen flow rates < 8.3 ml/minute (STP) and 0.3 ml/minute < hydrogen flow rates < 10.5 ml/minute (STP). Partial pressures were between 68 Pa < hydrogen < 500 Pa and 34 Pa < nitrogen < 270 Pa. The partial pressures are not directly proportional to the flow rates. This is because the pumping speed increases as the flow rates increase thereby decreasing the partial pressure. The resulting gas mixture was connected to the system by vacuum rubber tubing. The part of the system in contact with the microwave plasma was constructed out of quartz (fused silica) tubing.

The plasma was produced by a microwave cavity and power supply.[38] The cavity coupled the microwave radiation to the gases flowing through the quartz tube. The cavity was either a McCarroll[39] or Evenson microwave cavity[40] (Opthos Instruments). The experiments with platinum gauze were done with a McCarroll

cavity; subsequent experiments with rhodium utilized the Evenson cavity. The cavity is a hollow metal container with a shape and size allowing a standing electromagnetic wave to be established within it. The microwave generator (Opthos MPG-4) had a power range of 0-120 watts. The power was adjustable and the forward and reflected power to the cavity were measured. The frequency was 2450 MHz which is the standard frequency for microwave ovens. A Tesla coil was required to ignite the plasma. The optimal pressure in terms of power efficiency at a frequency of 2.45 GHz is approximately 540 Pa.[41]

A plasma, in this thesis, refers to the region in which the species are actually formed. In other words, this is the discharge itself which is characterized by intense luminosity and contains electrons, positively and negatively charged ions and atoms. Active nitrogen denotes the reactive species of a discharge in nitrogen.[42] For our purposes, we were more interested in the neutral species which have been excited electronically. Initially, a discharge is a result of randomly occurring free electrons being accelerated in the electric field until they gain sufficient energy to ionize some of the gas molecules. The electrons from this ionization are in turn accelerated and produce further ionization. This progressive effect causes extensive breakdown of the gas, the current rises and the discharge is established. Very soon a steady state is reached between the rate of formation of ions and the rate of their recombination. For pressures on the order of a few torr, this recombination occurs mainly on the walls of the quartz tubing.[41] As the flow rates for nitrogen and hydrogen increased so did the total pressure in the system. A third gas was not used to maintain constant pressure because it would affect the experiment in at least one of two ways. If a third gas was introduced prior to the microwave-induced plasma, it too would be electronically excited by the plasma and thereby provide additional routes for more intermediates.

For example if Ar was used, Ar would be excited to the $^2P_{0,2}$ state which when it reacts with ground state nitrogen preferentially produces the $^3\Sigma_u^+$ state of nitrogen. If the third gas was added after the plasma but before the catalyst, it would dampen the excited states present to lower excited states or to the ground state.

The quartz tubing was 13 mm in outer diameter in order to fit through the opening in the McCarroll and Evenson cavities. The catalysts were heated by means of two metal leads. These leads consisted of 1.4 mm diameter tungsten (Aesar 10412), 1.0 mm diameter tungsten (Aesar 10411) and 0.5 mm tantalum wire (Aesar 10349). The tantalum was spotwelded to the Rh(110) crystal and to the platinum gauze (Aesar 10283). The platinum gauze was a 52 mesh woven from 0.1 mm Pt wire. The Rh(110) crystal was characterized in quarterly reports by Ron Hendershot. A chromel-alumel thermocouple was spotwelded to the back of the Rh(110) crystal for temperature measurement. A side arm was provided on the Pyrex side of the apparatus for the thermocouple wire to be connected to the meter. Alumina sleeves were used to encase the tungsten wire. The single crystal was mounted perpendicularly to the gas flow to minimize reaction with the back side of the crystal and the tantalum leads.

The design of the glass in this region met four objectives: (1) allow catalyst heating, (2) permit catalyst temperature measurement, (3) provide for mechanical support for the catalyst, and (4) facilitate the ease of disassembly for modification and repair. A 9 mm O-ring seal was used to provide an easy way to connect and disconnect the catalyst from the rest of the system for easy cleaning and repair. (The platinum gauze setup had to be frequently cleaned due to the inadvertent formation of platinum films at higher hydrogen flow rates.) The 1.4 mm diameter tungsten leads entered the system through a uranium glass to provide proper sealing of the system as the tungsten leads were heated. A quartz to Pyrex graded seal was used for the gauze setup to join

the two portions of the system. For the Rh(110) work, a 5/8 inch Ultratorr fitting was used to connect the Pyrex and quartz portions. This was subsequently modified to accommodate 16 mm glass tubing. The Ultratorr fitting was used in order to facilitate repair and to allow the Rh(110) crystal to be mounted on the tantalum leads after the tungsten-uranium glass seals were annealed. The tungsten leads were of two different lengths to prevent electrical contact between the copper connectors which were used to join the tungsten and tantalum wire.

The Pyrex part of the system was necessary for the tungsten seal and the O-ring connection. Use of a microwave plasma requires quartz. A thermocouple pressure gauge was used to measure the pressure inside the system. A Pyrex trap cooled with liquid nitrogen was used to isolate the ammonia from the gas mixture of $N_2$, $H_2$, and $NH_3$ produced by this system. Connection to the mass spectrometer was made through a variable leak valve (Granville-Phillips, Model 203-012).

The mass spectrometer (UTI 100C) was used to monitor the contents of the trap. This unit operated in the mass range 1-300 mass/charge units and in the pressure range $10^{-6}$-$10^{-4}$ pascals. The product distribution of the species in the trap was recorded on a 2-channel oscillographic recorder (Hewlett-Packard, Model 7402A). The resolution of the mass spectrometer was improved for the 16, 17, and 18 m/e peaks by lowering the ionization energy to 12 V from 15 V. A concomitant loss in intensity of an order of magnitude for all peaks was observed. Since the mass spectrometric results show only relative differences in ammonia production, a calibration experiment was included. For two different sets of conditions, the same experiment was repeated the next day under identical conditions except that the contents of the trap were dissolved in distilled water, the volume measured, and a pH determination made. This pH determination was done

with a standardized pH meter which had been calibrated with a buffered pH 10.0 solution. The ammonia concentration was calculated by using a $K_b$ of $1.75 \times 10^{-5}$. This allowed for absolute ammonia concentrations to be measured and correlated with mass spectrometric results.

The nitrogen (99.998%) was obtained from Matheson Gas Products with a guaranteed hydrocarbon loading as $CH_4$ of less than 0.5 ppm. The hydrogen was Air Products Zero Hydrogen, 99.997% hydrogen. Both gases were purified by liquid nitrogen traps and gas purifiers (Matheson 6406) to remove oxygen. The nitric oxide (99.0%) was used without further purification.

## Kinetic Protocol

The procedure for the kinetic experiments reported in this thesis is as follows: First, the catalyst [Pt gauze or Rh(110)] was reduced by heating the catalyst to 300 degrees Centigrade in 270 Pa of flowing hydrogen overnight. Any exposure to air results in an extremely large decrease in ammonia production. Second, the liquid nitrogen traps were filled for the nitrogen and hydrogen gas lines. Third, the flow rates were adjusted to the desired values for the particular experiment, valves 1 and 3 opened and then the flow rates were checked for stability. Fourth, the microwave power supply was turned on to a forward power of 62 watts and the crystal temperature (usually 500 degrees Centigrade)was adjusted, if necessary. Fifth, once the system had stabilized for flow rates, crystal temperature, and power level, the ammonia collection trap was cooled with liquid nitrogen. Sixth, the timer was started, the trap refilled with liquid nitrogen when necessary and all parameters checked and adjusted, if necessary, at two minute intervals. Seventh, valve 2 was opened and the mass spectrum of the reactants checked. Eighth, at the end of two hours, valve 1 was closed

and the system was pumped out except for the frozen contents of the trap. Ninth, valve 3 was closed and the trap warmed to ambient temperature. Finally, mass spectra and total pressure readings were collected.

## Spectroscopic Analysis

As shown in Figure 2, the design of the spectroscopic analysis system is very similar to the kinetic system. In place of the catalyst, a monochromator slit is seen on the outside of the quartz tube. A Jarrell-Ash (Model 52-410) monochromator was used. A photomultiplier tube was connected to the monochromator and also to the autoranging picoammeter (Keithley 485). This in turn was interfaced through an IEEE-488 bus to a microcomputer (PDP-LSI11/23). The operating language was RT-11, version 5.4. A program was written for data acquisition with suggestions from a sample program provided by Keithley. In a typical run, 17 measurements were averaged per nanometer and stored. The autoranging feature of the picoammeter was crucial for the uninterrupted collection of data, since in the course of collecting one spectrum, the range was changed an average of five times. Spectra were taken of the plasma afterglow for varying nitrogen/hydrogen gas mixtures. The wavelengths were calibrated with a mercury lamp.

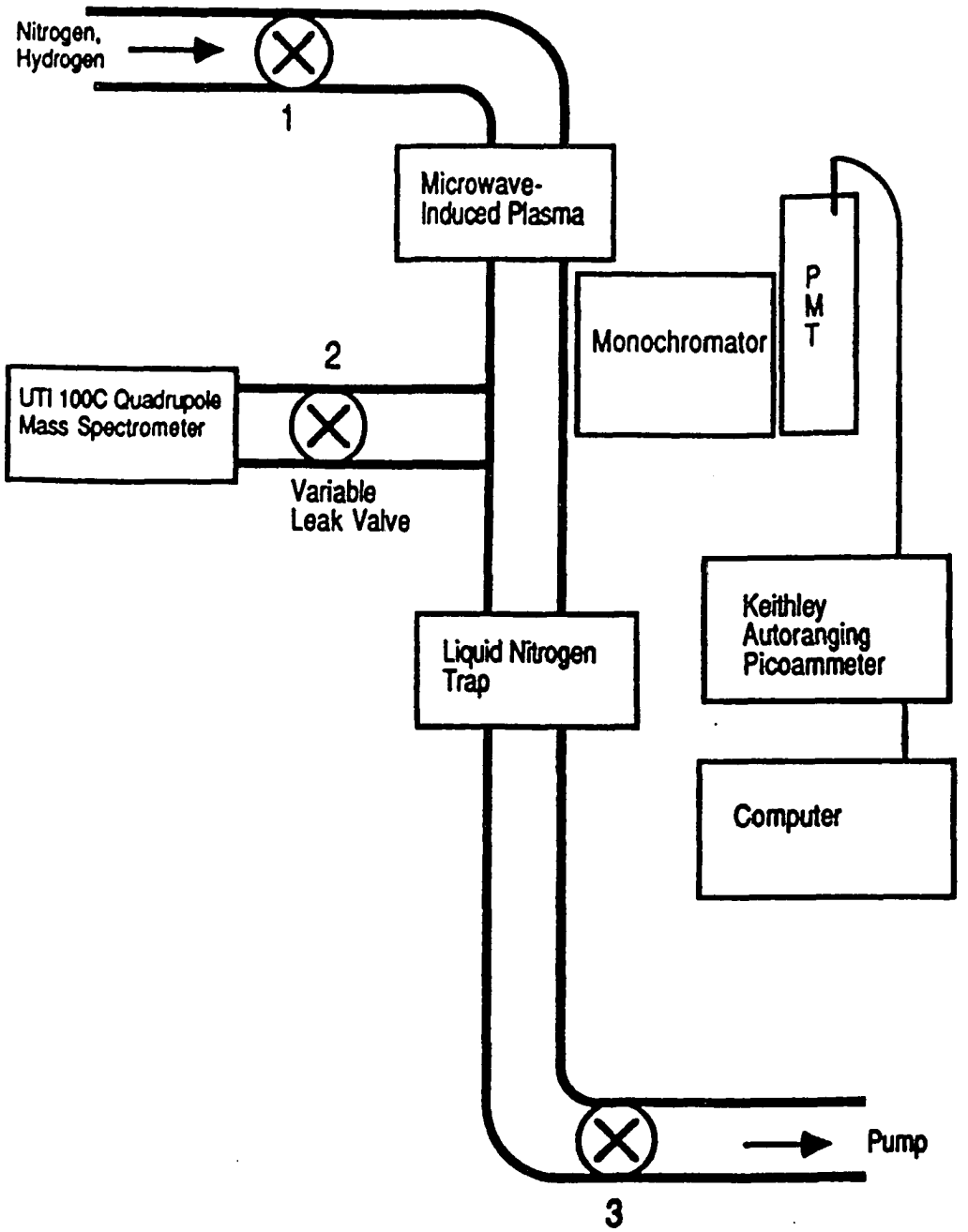


Figure 2. A schematic of the spectroscopic analysis system

## Atomic Nitrogen Titration

As will be shown in a later section, spectroscopic results for the detection and quantitation of atomic nitrogen were inconclusive. Therefore, a second method was chosen to provide this information. Mass spectroscopy was considered and discarded as a method because of the large amount of molecular nitrogen in the system and the molecular nitrogen fragmentation pattern which includes 14 m/e$^-$. Mass spectroscopy with the instrument available would not give a definitive result. The method of choice was a gas phase titration of atomic nitrogen with nitric oxide.[28,43,44] Visual observation can be used to mark the endpoint. The visual endpoint consists of a change from blue to green as the concentration of nitric oxide is increased. The equivalence point has virtually no emission. Before the equivalence point, the following reactions describe what is occurring in the afterglow.

$$N + NO \rightarrow N_2 + O \qquad k_1 = 2\times10^{-11}\ cm^3 molecule^{-1} sec^{-1} \text{(ref. 44)} \qquad [1]$$

$$N + O + M \rightarrow NO^* + M \qquad k_2 = 3\times10^{-32} cm^6 molecule^{-2} sec^{-1} \text{(ref. 45)} \qquad [2]$$

The net reaction is

$$2N + NO \rightarrow N_2 + NO^*$$

After the equivalence point the behavior of the afterglow is described by these reactions:

$$N + NO \rightarrow N_2 + O \qquad k_3 = 2\times10^{-11}\ cm^3\ molecules^{-1} sec^{-1}\ \text{(ref. 44)} \qquad [3]$$

$$O + NO \rightarrow NO_2^* \rightarrow NO_2 + h\nu \qquad [4]$$

$$k_4 = 2.5\times10^{-17} cm^3 \text{ molecules}^{-1}\text{sec}^{-1} \text{ (ref. 45)}$$

The net reaction after the equivalence point is:

$$N + 2NO \rightarrow NO_2^* + N_2 \rightarrow NO_2 + N_2 + h\nu$$

In conclusion, before the equivalence point, the oxygen atoms produced by the first reaction react to form $NO^*$; therefore the production of NO* is predominant and results in the blue emission seen. After the equivalence point, the oxygen atoms produced by the first reaction form $NO_2^*$ resulting in a greenish-yellow emission. Mathematically, this can be represented by

$$[NO^*]_{rate}/[NO_2^*]_{rate} = k_2C_NC_OC_M/k_4C_OC_{NO}$$
$$= k_2C_NC_M/k_4C_{NO} \approx kC_N/C_{NO}$$

where before the equivalence point $C_N >> C_{NO}$ and the production of $NO^*$ is enhanced and after the equivalence point $C_{NO} >> C_N$ formation of $NO_2^*$ is favored so the color changes. At the equivalence point, all the atomic nitrogen reacts with nitric oxide to produce molecular nitrogen and oxygen atoms, therefore no emission due to $NO^*$ or $NO_2^*$ is seen.[27]

The spectroscopic analysis setup was modified for the atomic nitrogen titration by the inclusion of a sidearm between the plasma and the monochromator slit through which nitric oxide was introduced. A variable leak valve (Granville-Phillips, Model 203-012) controlled the flow rate of the NO. A second gas regulator (Scott Model 23) for reduced pressure was used in series with the gas regulator on the nitric oxide tank to allow a backing pressure of 1 psi which decreased the flow rate of the NO through the

variable leak valve. The pressure of nitric oxide was measured by a thermocouple gauge mounted near the trap. The signal from the ultraviolet-visible spectrometer at 237 nm was used to determine the endpoint. This spectral line is associated with the $NO^*$ formed before the equivalence point for the titration.[46] For each determination of atomic nitrogen, the flow rates of nitrogen and hydrogen were held constant. The NO pressure was varied as the intensity of the 237 nm line was measured. When the intensity of that line reached baseline as the NO pressure was increasing, the NO pressure for that behavior was labelled as the endpoint for the titration. A series of intensity measurements for the 237 nm line for a range of NO pressures was done for each determination of atomic nitrogen for to accurately determine a baseline for each gas mixture. For the best correlation between ammonia production and atomic nitrogen pressure, the following protocol was observed. The monochromator slit was 33 mm from the edge of the Evenson microwave cavity, the same position used for the rhodium single crystal. The sidearm for the nitric oxide was 10 mm from the edge of the cavity and 23 mm from the monochromator slit. This provided for thorough mixing of the atomic nitrogen and nitric oxide and in addition, prevented the nitric oxide from interacting with the plasma.

# RESULTS

The presence of atomic nitrogen is the most interesting facet of these results. Without the mediating presence of the microwave plasma, ammonia is not produced under these conditions. Therefore, ground state molecular nitrogen can be ruled out as a precursor. All attention must be focused on the characterization of the plasma and the corresponding relationship between the amount of atomic nitrogen produced and the production of ammonia.

## Spectroscopic Results

Examination of the afterglow by emission spectroscopy was the first step in the characterization of the species produced in the plasma. Due to the complexity of the initial spectra, a glass wool plug was inserted in the region of the afterglow immediately after the plasma to quench the shorter lived transient species and simplify the spectrum. As a consequence of introducing the glass wool into the system, the sodium peak increases dramatically in intensity. The resulting emission spectra were suitable for analysis. All emission is from excited species produced by the microwave cavity. For all spectra analyzed, the forward power applied to the microwave cavity was 60 watts and the reflected power was 10 watts. All spectra were carefully analyzed for the emission line from atomic nitrogen transition corresponding to the $N(^2P \rightarrow ^4S)$ at 346 nm, but it was not observed under the given experimental conditions.[47,48] This can be attributed to the weakness of the emission for this transition and to presumably small quantities produced in the plasma. The four spectra shown in Figures 3-6 which

are the most informative are shown on the following pages with their accompanying tables of identified peaks. As can be seen, all major peaks were attributed to molecular nitrogen, atomic hydrogen or sodium. NH and $NH_2$ were not produced in the apparatus as described earlier in Figure 2 for 1.6 ml/minute nitrogen flow rate (180 Pa), hydrogen flow rates between 1.3 and 4.5 ml/minute (250-680 Pa), and a forward power of 62 watts. The NH ($b^1\Sigma^+$) state has been produced by the vacuum photolysis of $NH_3$ while NH ($A^3\Pi$) can be produced by the interaction of Ar or Kr with $NH_3$.[48] $NH_2$ has been produced by multiphoton dissociation of $NH_3$.[49]

Since the emission at 347 nm from the $^2P$ to the $^4S$ ground state of atomic nitrogen was not seen and the $^3\Sigma_u^+$ state results from the recombination of ground state N ($^4S$) atoms and is also formed directly by the plasma, neither set of emission lines, the $^2P \rightarrow {}^4S$ or the $B^3\Pi_g \rightarrow A^3\Sigma_u^+$offers an unambiguous method for the measurement of atomic nitrogen pressure. Therefore, we decided to use the gas-phase nitric oxide titration of atomic nitrogen to elucidate the atomic nitrogen pressures. However, qualitative data on other species were obtained by emission spectroscopy.

The first step in the identification of species present in the afterglow was to look at the transients produced separately in a hydrogen plasma and a nitrogen plasma. The plasma ignited in pure nitrogen was found to contain small amounts of oxygen and sodium. A nitrogen flow rate of 1.6 ml/minute (180 Pa) was employed. A molecular sieve was found to greatly reduce the oxygen concentration; due to the sensitivity of emission spectroscopy, peaks attributed to oxygen were still seen although no products containing oxygen were observed in the mass spectra of the products. Both the 1st and 2nd positive bands of nitrogen are observed in the emission spectra shown in Figure 3. The 1st positive band corresponds to the transition $B^3\Pi_g \rightarrow A^3\Sigma_u^+$ and the 2nd

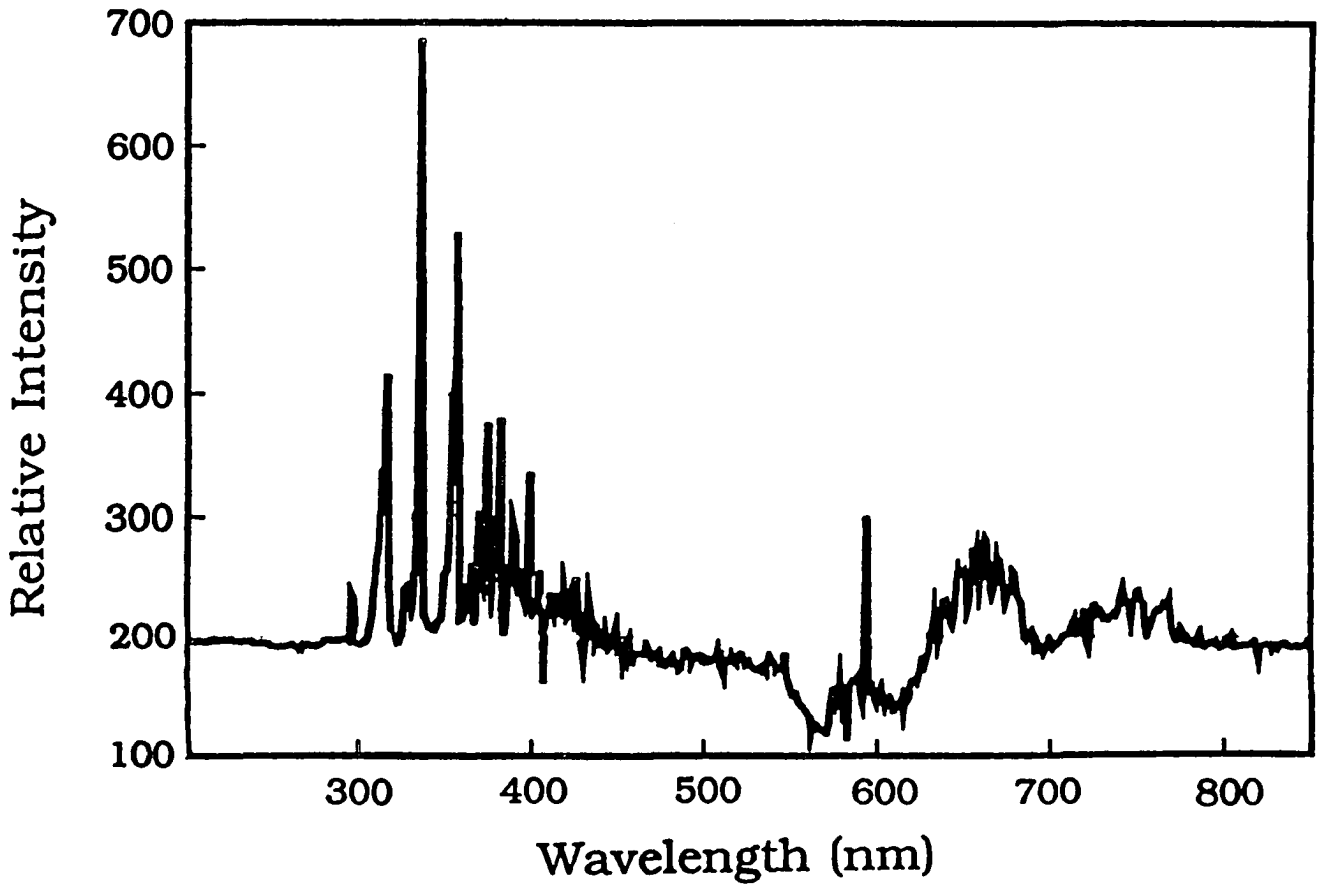


Figure 3. Spectrum of afterglow for a nitrogen flow rate of 1.6 ml/minute (180 Pa)

positive band results from the $C^3\Pi_u \rightarrow B^3\Pi_g$ transition. For the manifold of excited states the $A^3\Sigma_u^+$ state is the longest lived with a lifetime of 2 seconds.[48] The $N_2(B\ ^3\Pi_g)$ is the shortest with a lifetime of 8 milliseconds.[48] The N ($^4S$) recombines with a rate constant of $0.96 \times 10^{-32}$ $cm^6/molecules^2sec$ for $-k[N(^4S)]^2[M]$ where M is a gas species to take up the energy released by the recombination.[50]

For flow rates of 4.5 ml/minute hydrogen (680 Pa) as shown in Figure 4, two of the three strong atomic hydrogen peaks are seen at 656 and 486 nm and sodium peak at 589 nm. The hydrogen peaks are characteristic for both excited molecular hydrogen and atomic hydrogen. Differentiation between these two species is impossible under these circumstances because the emission from excited molecular hydrogen has few characteristic features. The rotational structure is so open that there are no heads or close groups of lines to form the usual band structure.[46] The hydrogen plasma did not require ignition by a Tesla coil.

The third spectrum shown in Figure 5 approximates a simple addition of the previous two spectra. Hydrogen flow rate is 1.3 ml/minute (250 Pa) and the nitrogen flow rate is 1.6 ml/minute (180 Pa). The less intense nitrogen 1st positive bands however are no longer seen when hydrogen is introduced into the plasma.[27] The same vibrational levels, $v' = 0,1,2$ (associated with the $C\ ^3\Pi_u$ state) and $v''=0,1,2,3,4$ ($B\ ^3\Pi_g$ states), are populated for the nitrogen-hydrogen mixture, as for the nitrogen spectrum alone. The fourth spectrum is for the case where the hydrogen flow rate of 4.5 ml/minute (680 Pa) was approximately 3 times the nitrogen flow rate of 1.6 ml/minute (180 Pa) and is illustrated in Figure 6. Again the nitrogen 2nd positive band is observed but additional vibrational levels, the $v''=5,6$, and 7 and the $v'=3$ were seen

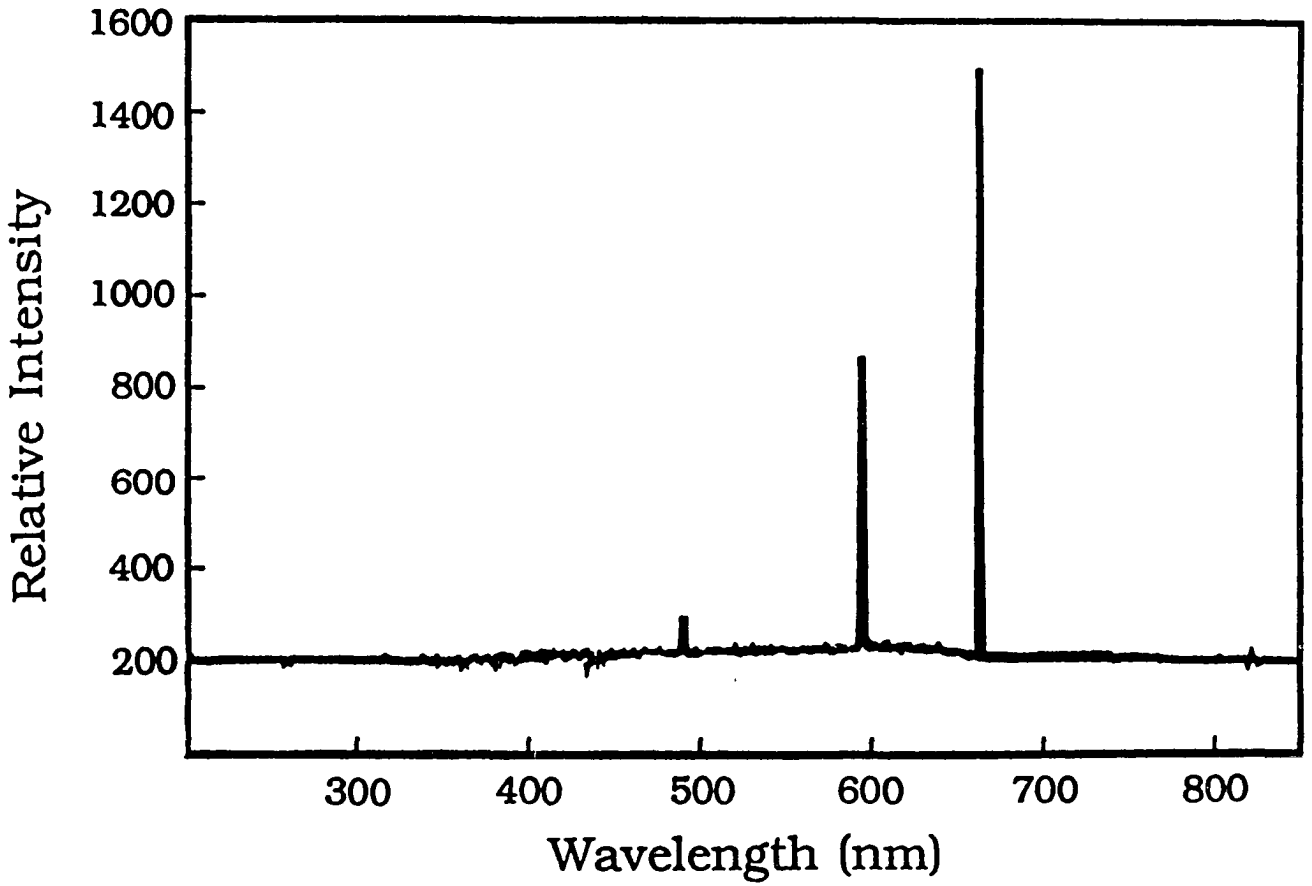


Figure 4. Spectrum of afterglow for a hydrogen flow rate of 4.5 ml/minute (680 Pa)

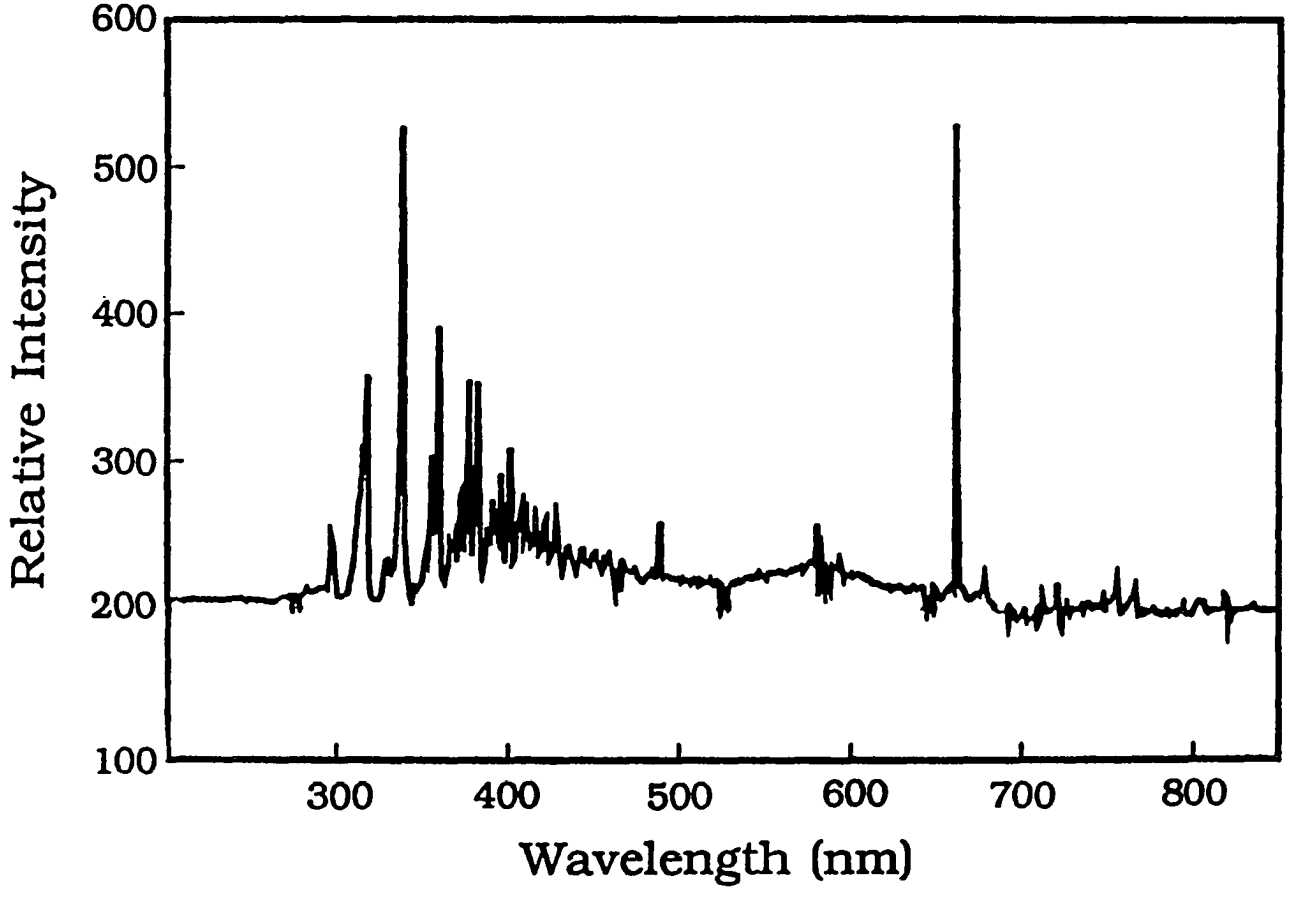


Figure 5. Spectrum of afterglow for a nitrogen flow rate of 1.6 ml/minute (180 Pa) and hydrogen flow rate of 1.3 ml/minute (250 Pa)

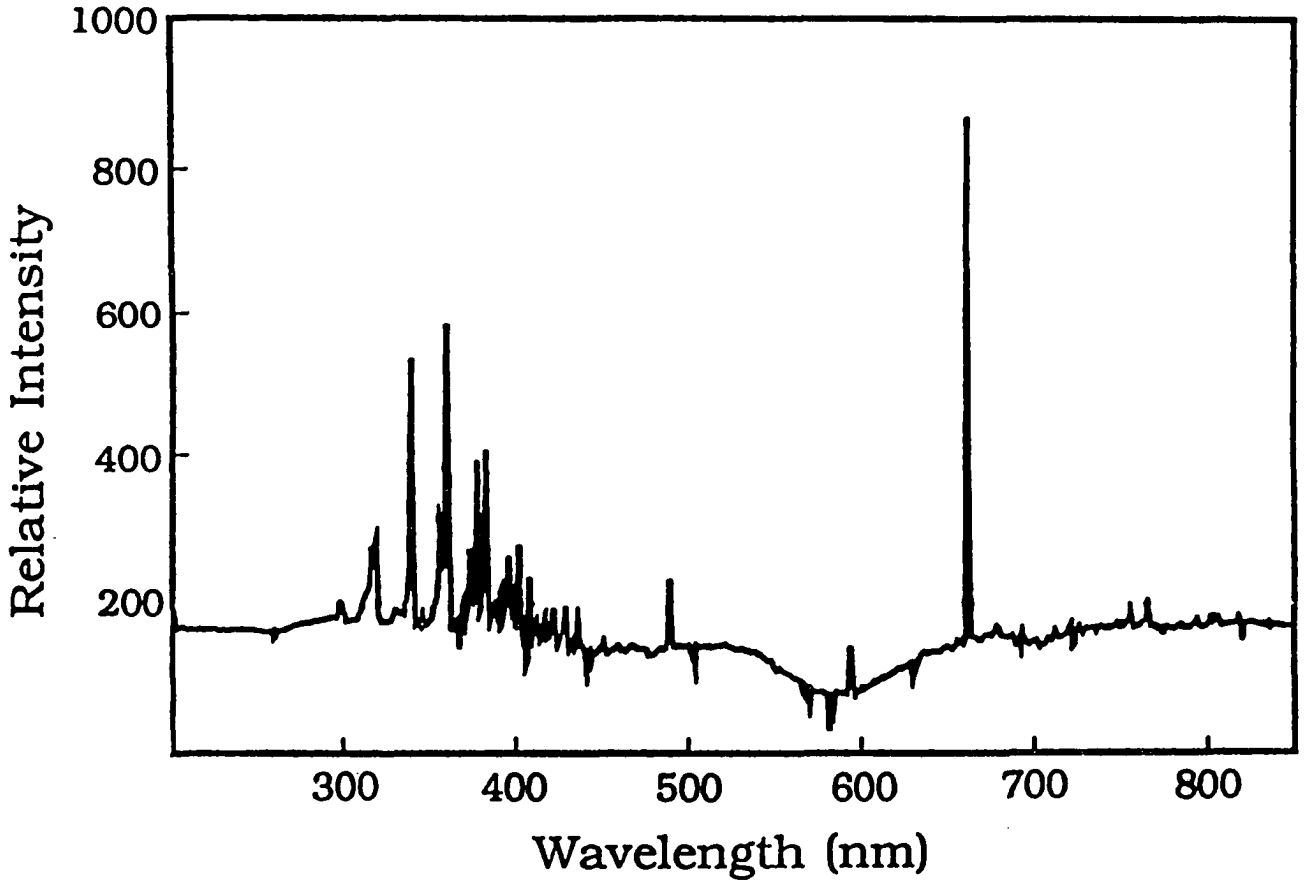


Figure 6. Spectrum of afterglow for a nitrogen flow rate of 1.6 ml/minute (180 Pa) and hydrogen flow rate of 4.5 ml/minute (680 Pa)

for this case. This is apparently due to increased collisions of the atomic hydrogen with nitrogen, which transfers energy to the molecular nitrogen and increases the number of vibrational states observed. This is consistent with atomic nitrogen titration results showing enhanced dissociation of nitrogen for higher hydrogen flow rates.

## Atomic Nitrogen Determination

The first atomic nitrogen determination was done for the system containing platinum gauze and was done in order to verify that the ammonia produced was dependent on the atomic nitrogen pressure before proceeding to a single crystal catalyst. The calibration of atomic nitrogen pressure versus molecular nitrogen pressure is dependent on the dimensions of the discharge tube and is shown in Figure 7. The atomic nitrogen pressure reaches a maximum for a nitrogen flow rate of 3.0 ml/minute (130 Pa) at a constant hydrogen pressure of 280 Pa and flow rate of 1.6 ml/minute. The atomic nitrogen then decreases for increasing molecular nitrogen pressures. The decrease in pressure is attributed to the shorter lifetime of atomic nitrogen at higher total pressures. Because of the sensitivity of the atomic nitrogen calibration to the dimensions of the glass tubing, the calibration was repeated for the flow system containing the Rh(110) crystal. Figure 8 shows the dependence of atomic nitrogen on molecular nitrogen pressure when the hydrogen pressure is kept constant at 450 Pa (2.8 ml/minute). The atomic nitrogen pressure increases as the nitrogen pressure increases. The dependence of atomic nitrogen on hydrogen pressures is shown in Figure 9 and displays an interesting behavior. As the hydrogen pressure is increased and the nitrogen pressure is maintained at 220 Pa (flow rate of 2.1 ml/minute), the atomic nitrogen pressure increases in a linear fashion. This proportionality has also been seen for $SF_6$

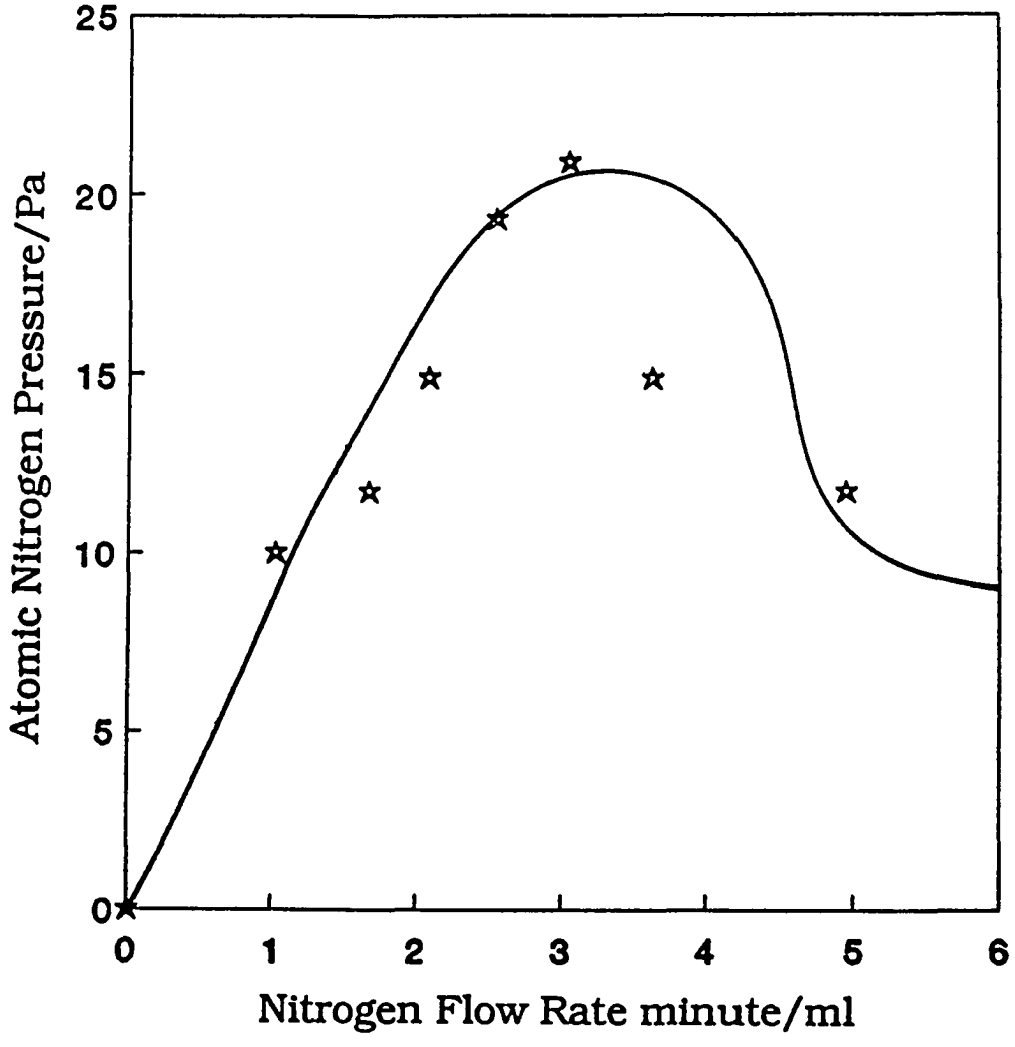


Figure 7. Atomic nitrogen dependence on nitrogen flow rate with the hydrogen flow rate held constant at 1.6 ml/minute (280 Pa). This calibration is for the system containing Pt gauze

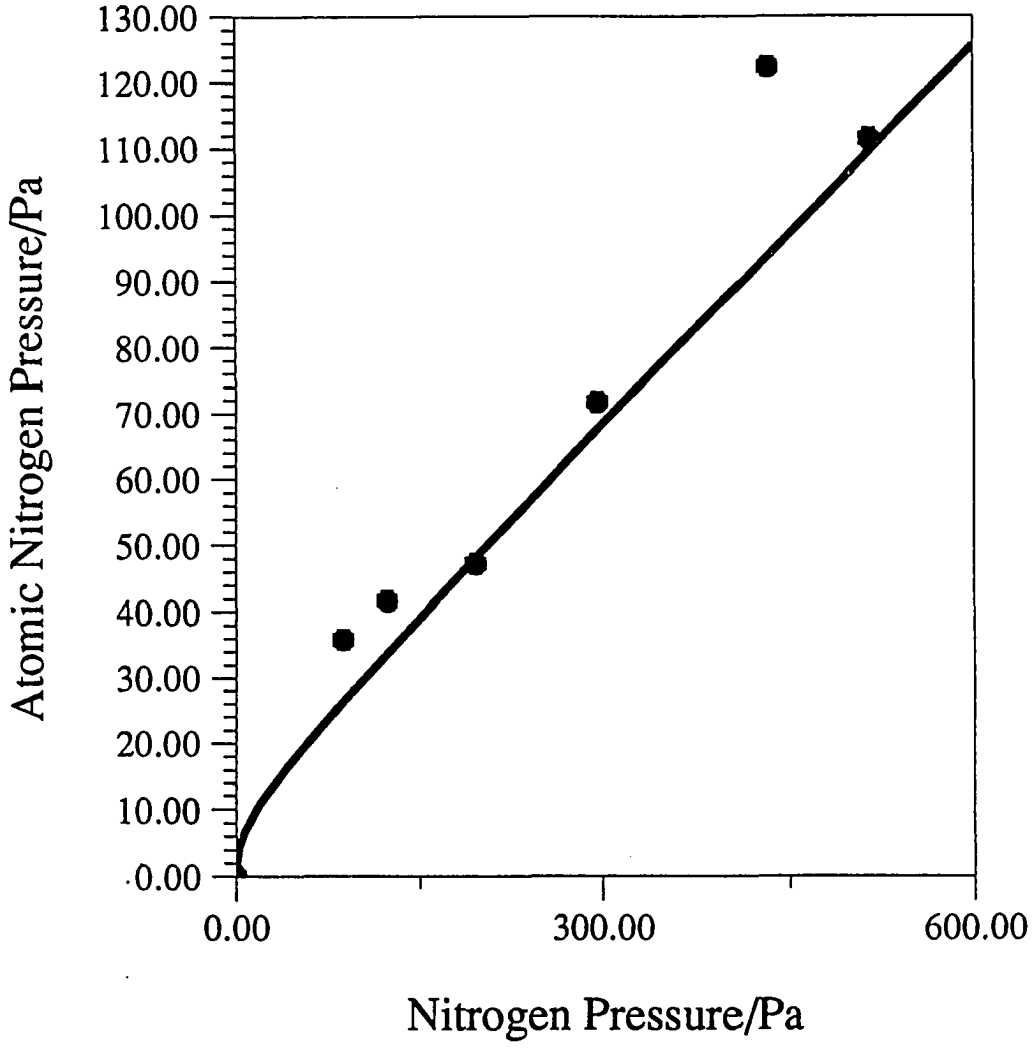


Figure 8. Atomic nitrogen dependence on nitrogen flow rate with the hydrogen pressure held constant at 450 Pa (2.8 ml/minute). This calibration is for the system containing the Rh(110) crystal. The squares represent the actual data; the line is from the model described in the text

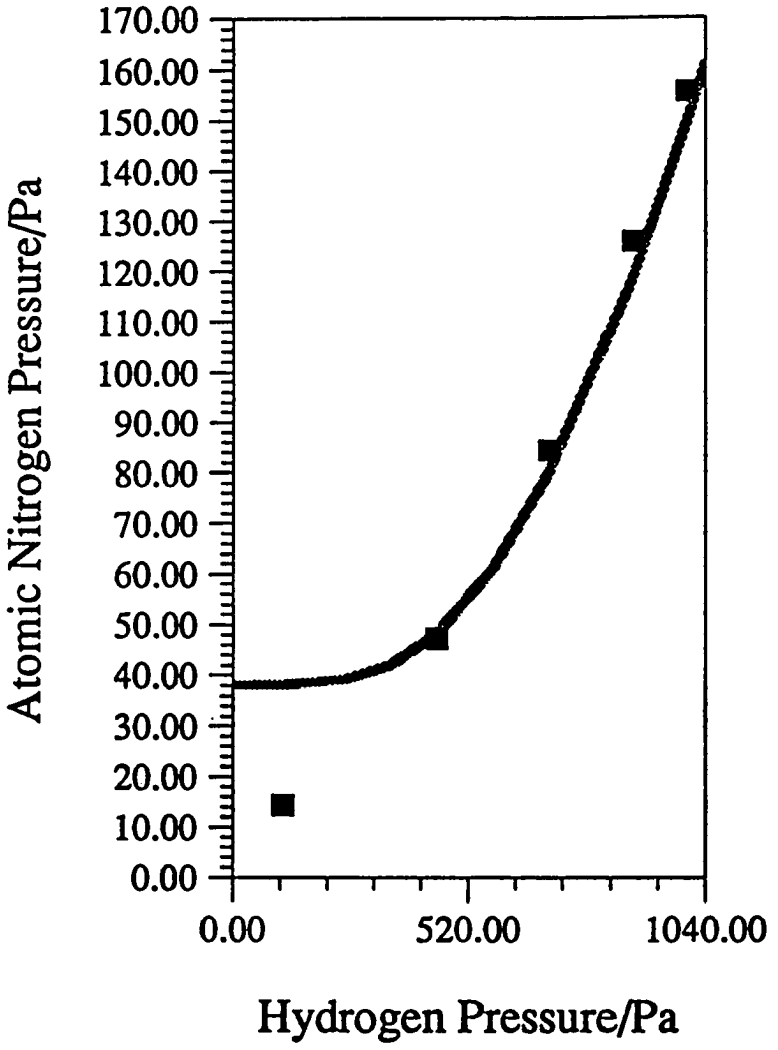


Figure 9. Atomic nitrogen dependence on hydrogen flow rates with the nitrogen pressure held constant at 220 Pa (2.1 ml/minute). This calibration is for the system containing the Rh(110) crystal. The squares represent the actual data; the line is from the model described in the text

concentrations varying from 50-500 ppm added to a nitrogen flow of 50 ml/minute in a microwave discharge, resulting in a tripling of the nitrogen dissociation observed from 2 to 6%.[51] Gas phase collisions of excited hydrogen with nitrogen result in increased energy transfer to the molecular nitrogen causing more dissociation to occur. The intercept for this line is nonzero because the atomic nitrogen is formed in a microwave induced plasma without hydrogen present.

## Kinetic Rates

Another crucial piece of evidence in elucidating the mechanism of ammonia formation from hydrogen and atomic nitrogen is the dependence of ammonia formation rates on reactant pressures. For the platinum gauze apparatus, the rate of ammonia production is proportional to the nitrogen flow rate as shown in Figure 10. The hydrogen flow rate was held constant at 1.60 ml/minute and a hydrogen partial pressure of 280 Pa. The nitrogen flow rates were varied 0.76 and 3.2 ml/minute which corresponds to nitrogen partial pressures between 120 and 310 Pa, respectively. The rate of ammonia formation was proportional to the pressure of ammonia in the mass spectrometer. An ammonia pressure of $4.41 \times 10^{-5}$ Pa has been arbitrarily set equal to a rate of 10.0. This means that the $[P_{NH_3}]_{\text{mass spectrometer}} = k_1[P_{NH_3}]_{\text{reaction system}} = k_2 k_1$[reaction rate][time] but that $k_1$ and $k_2$ are unknown for this experiment. All other rates were calculated based on this calibration for Figures 10 and 11.

As described earlier in the kinetic protocol, the forward power was set equal to 62 watts for all the results. The one exception is Figure 11. Figure 11 shows the rate of ammonia formation as a function of power supplied to the microwave plasma in a flow system using a Pt gauze catalyst. The nitrogen flow rate was held constant at

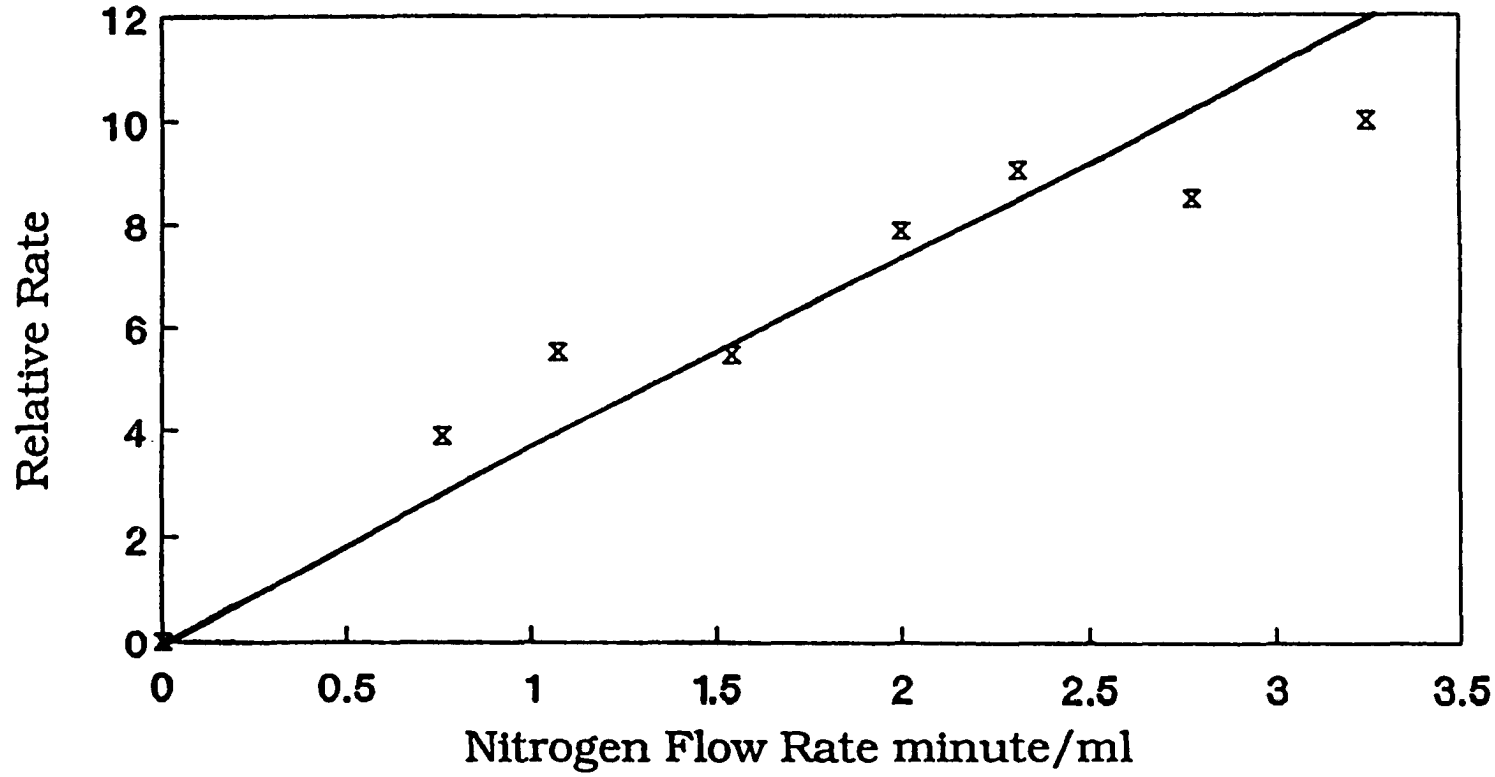


Figure 10. Rate of ammonia production as a function of nitrogen flow rate for a Pt gauze catalyst at a constant hydrogen flow rate of 1.6 ml/minute (370 Pa)

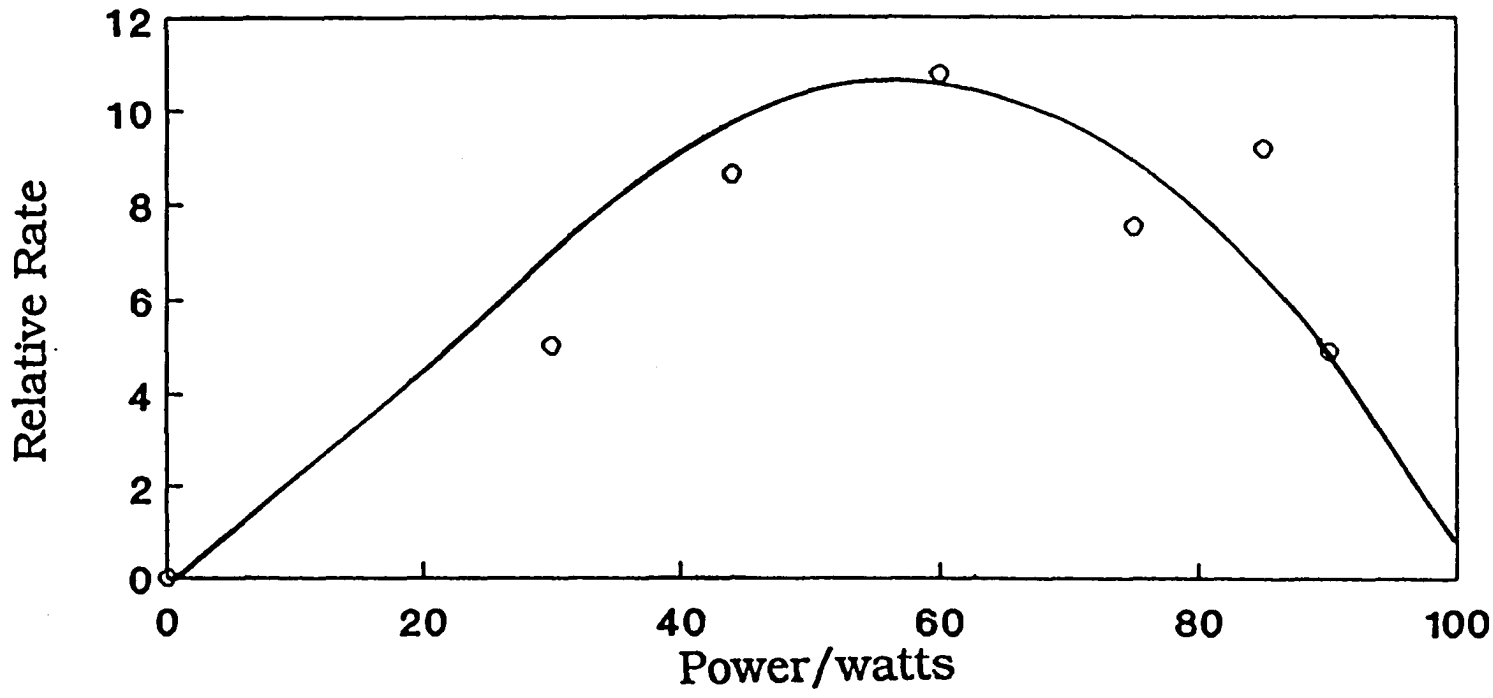


Figure 11. Rate of ammonia production as a function of forward power supplied to the microwave plasma for a Pt gauze catalyst

1.5 ml/minute ($P_{N_2}$ = 170 Pa) and the hydrogen flow rate at 2.1 ml/minute ($P_{H_2}$ = 340 Pa). The platinum gauze was heated to a temperature of 500° C. The results at the extremes were difficult to obtain since the microwave cavity required extensive retuning to produce a stable plasma. Power levels below 30 watts were insufficient to maintain a plasma while power levels above 90 watts were not investigated because the reflected power exceeded safe levels for the operation of the microwave plasma. The maximum rate of ammonia production occurred at a forward power of approximately 60 watts.

The rates of ammonia formation as a function of reactant pressures utilizing Rh(110) as a catalyst, show similar behavior to those obtained for Pt gauze. The rate of ammonia formation as a function of nitrogen pressure between 100 and 570 Pa (flow rates between 0.5 and 8.3 ml/minute) is illustrated in Figure 12. As mentioned in the experimental section, the pressures do not increase proportionally with flow rates because of changes in pumping speed for higher flow rates. The rate reaches a maximum at a nitrogen pressure of 430 Pa (flow rate of 5 ml/minute) and decreases slowly for higher nitrogen pressures. The hydrogen pressure was held constant at 450 Pa (flow rate of 2.8 ml/minute). Figure 13 is the corresponding result for variations in hydrogen pressures between 110 and 1000 Pa (flow rates between 0.3 and 10 ml/minute) with the nitrogen pressure held constant at 220 Pa (flow rate of 2.1 ml/minute). This graph shows that the rate of ammonia production is proportional to the hydrogen pressure. In both cases for nitrogen and hydrogen pressures, the rates of ammonia formation can be explained by the rate of atomic nitrogen formation. A model for this behavior has been made by assuming the rate of atomic nitrogen formation is as follows:

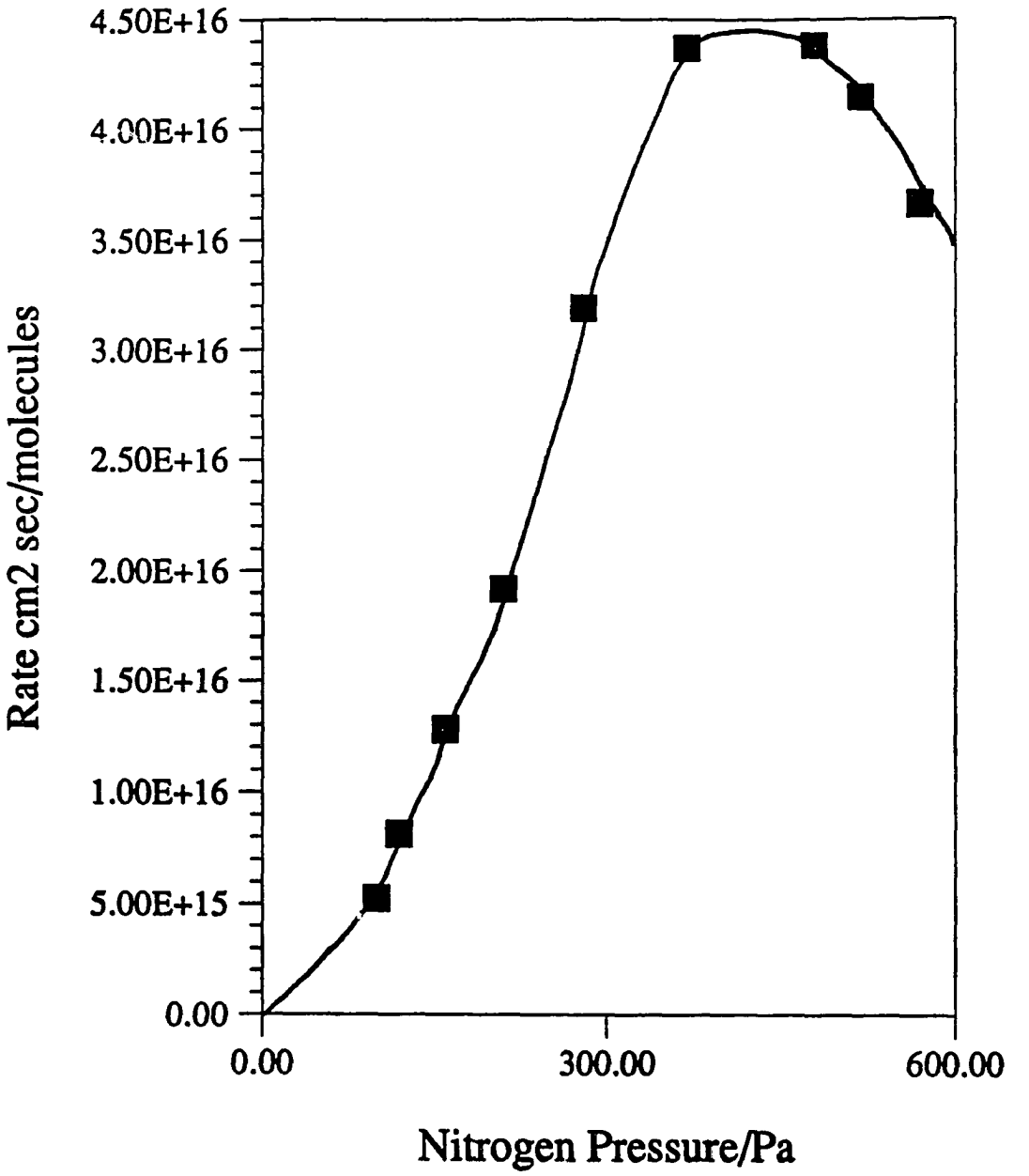


Figure 12. Rate of ammonia production as a function of nitrogen pressure for a Rh(110) catalyst at a constant hydrogen pressure of 450 Pa

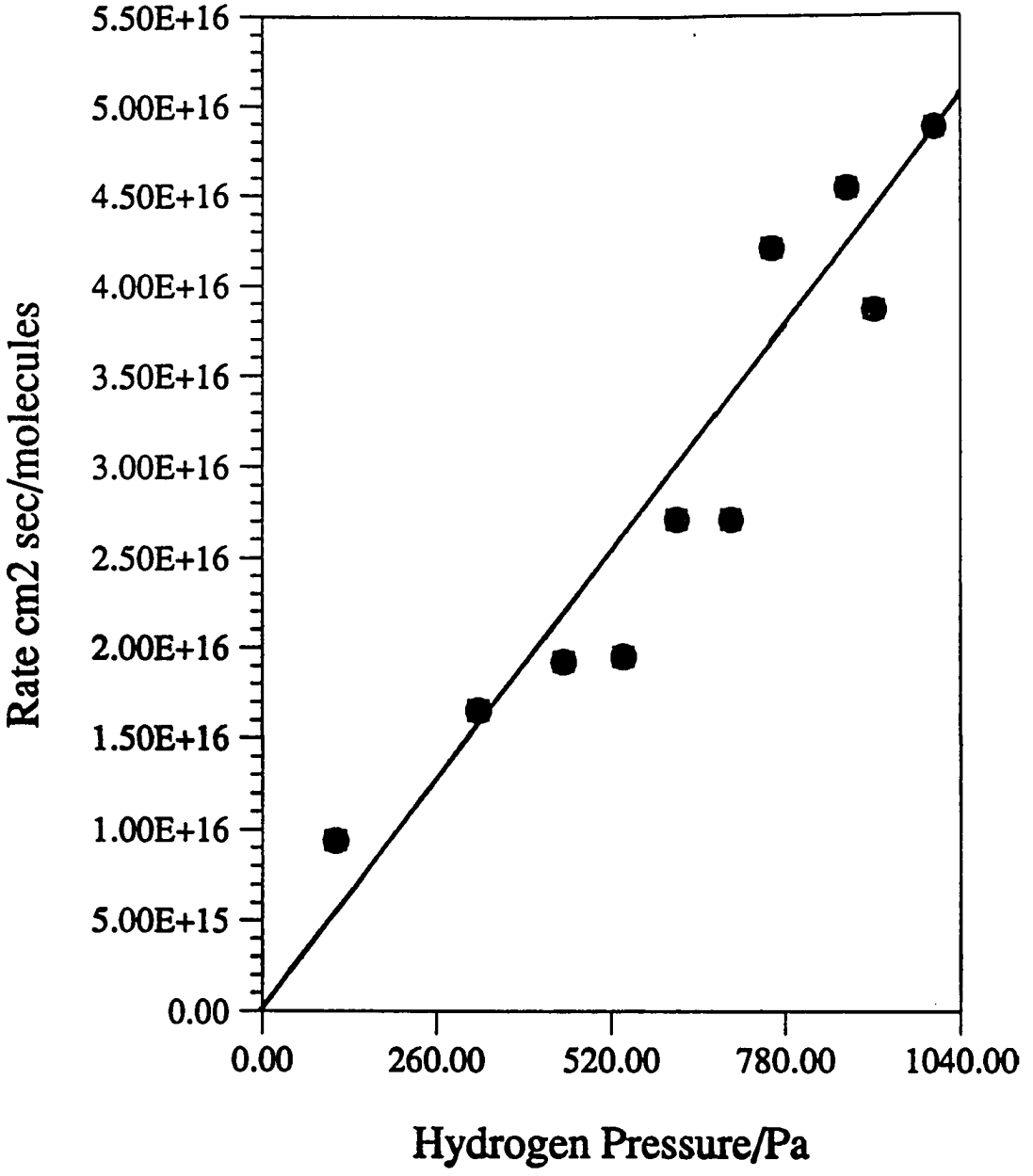


Figure 13. Rate of ammonia production as a function of hydrogen pressure for a Rh(110) catalyst at a constant nitrogen pressure of 220 Pa

$$(dP_N/d\tau)_{formation} = (k_1 P_{N_2} + k_2 P_{H_2}{}^4) P_{N_2} \quad (1)$$

The dissociation of nitrogen to atomic nitrogen requires 10 eV and the total excitation necessary to provide this energy might be more easily achieved from the interaction of a number of excited molecules than from a single excited molecular nitrogen species. The first term refers to the proportional dependence on the square of the pressure of the molecular nitrogen. The second term postulates that the energy transfer from hydrogen to nitrogen also results in the dissociation of nitrogen. The rate of atomic nitrogen removal is represented by the following:

$$(dP_N/d\tau)_{removal} = - k_3 P_N{}^2 \quad (2)$$

The rate for atomic nitrogen removal is well known to be a three body process for the gas phase. For our model, the primary means of removal occurs with the wall acting as the third body resulting in the $k_3 P_N{}^2$ term. By assuming a steady state, $(dP_N/d\tau)_{formation} + (dP_N/d\tau)_{removal} = 0$, the resulting equation can be solved for:

$$P_N = P_{N_2}{}^{0.5} (k_1/k_3 P_{N_2} + k_2/k_3 P_{H_2}{}^4)^{0.5} \quad (3)$$

The lines drawn in Figures 8 and 9 correspond to this fit for values of $k_1/k_3 = 0.030$ and $k_2/k_3 = 9.5 \times 10^{-11}$ $Pa^{-3}$.

### Correlation of Rates and Atomic Nitrogen Pressures

From results presented earlier in the results section, the relationship between the atomic nitrogen pressure and the flow rate is known. Combining this information with the rate dependence on the nitrogen flow rate allows one to determine the dependence of ammonia production rate on the atomic nitrogen pressure. This was done for the Pt

gauze catalyst as shown in figure 14. This results in a straight line or in other words, the rate of ammonia production is proportional to the atomic nitrogen pressure. This proportionality demonstrates that the earlier 'apparent dependence' of ammonia production on nitrogen flow rate is actually a dependence on the atomic nitrogen pressure.

The same procedure was repeated for the Rh(110) data. Figure 15 shows the results of this calculation for nitrogen pressures. The rate is again, at least approximately, proportional to the atomic nitrogen pressure. The corresponding data for variations in hydrogen pressures is shown in Figure 16. The same dependence is observed.

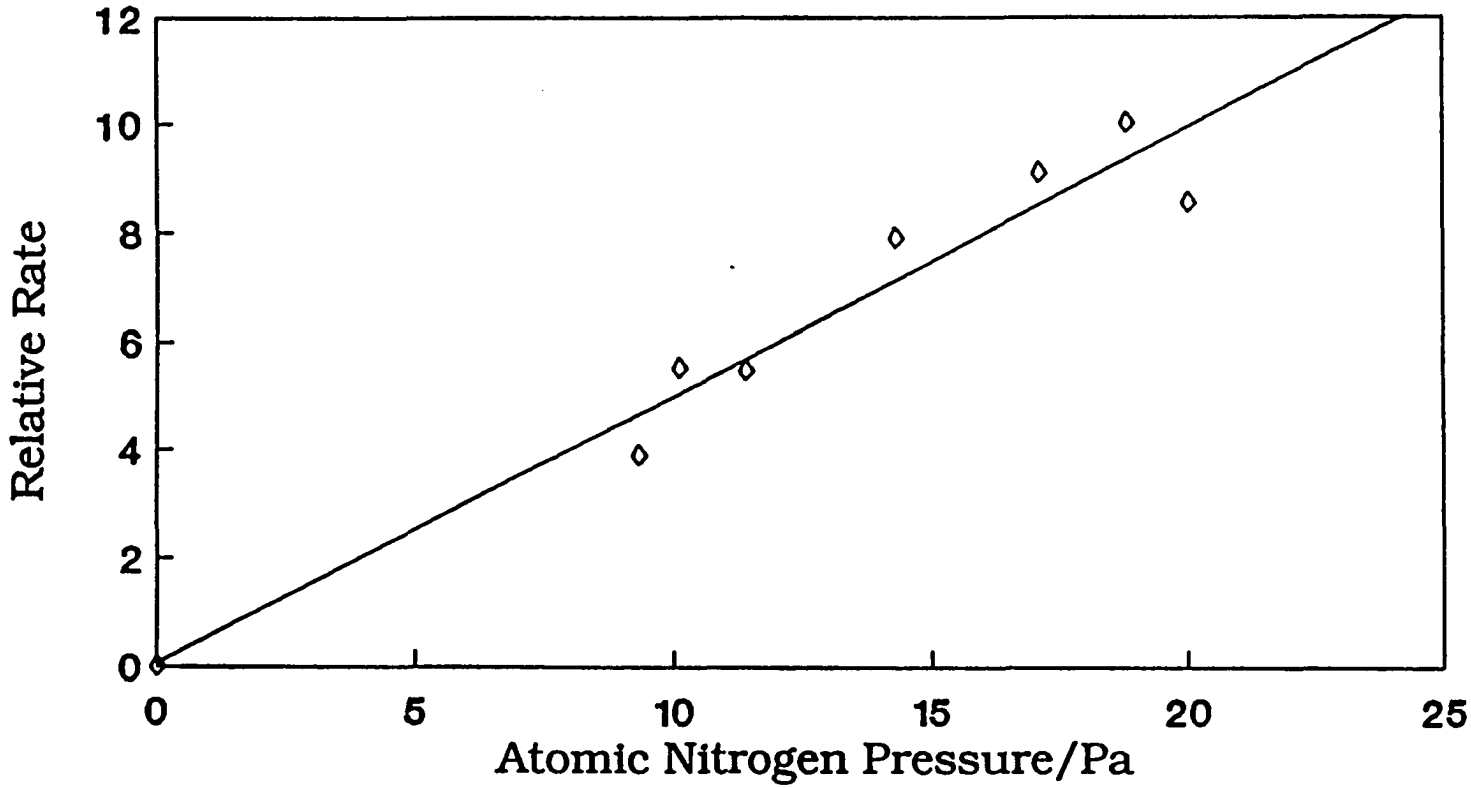


Figure 14. Dependence of the rate of ammonia production on atomic nitrogen pressure at a constant hydrogen flow rate of 1.6 ml/minute for a Pt gauze catalyst. (280 Pa)

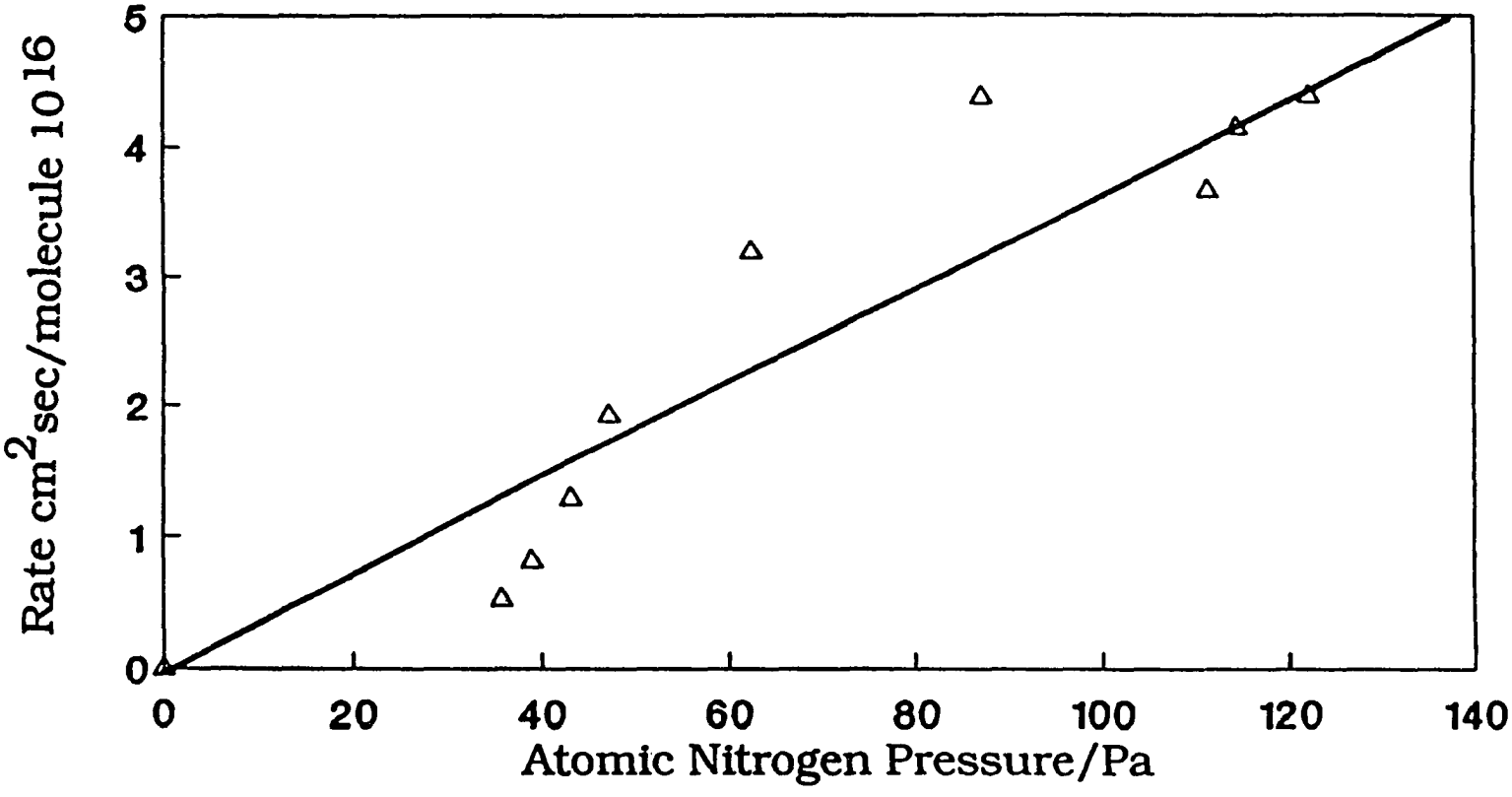


Figure 15. Dependence of the rate of ammonia production on atomic nitrogen pressure at a constant hydrogen pressure of 450 Pa for a Rh(110) catalyst

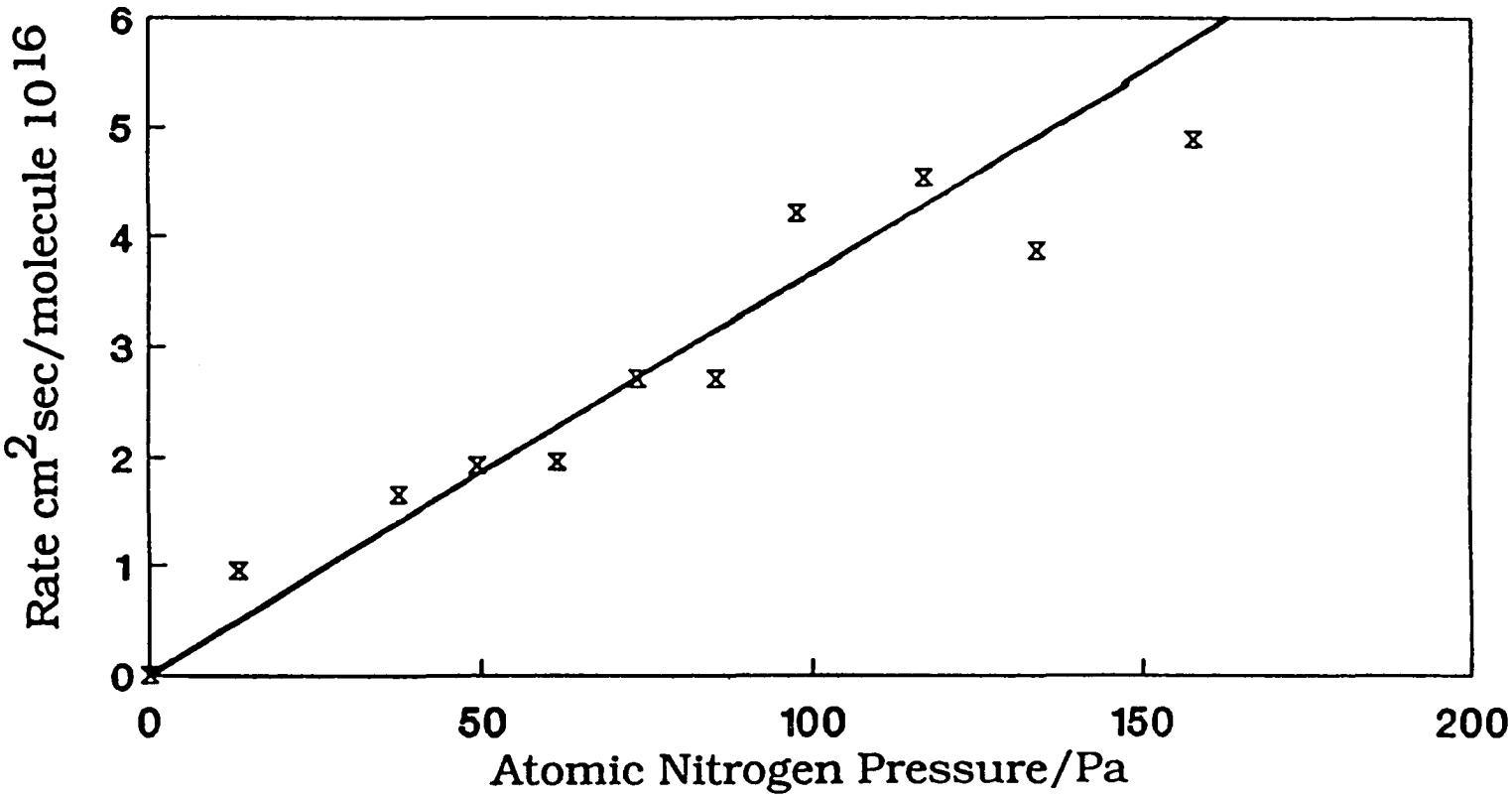


Figure 16. Dependence of the rate of ammonia production on atomic nitrogen pressure at a constant nitrogen pressure of 220 Pa for a Rh(110) catalyst

# DISCUSSION

In order to explain the results presented earlier, a rate mechanism consisting of atomic nitrogen adsorption, reaction of the adsorbed species and its subsequent formation of ammonia or recombination is shown. The effect of temperature on the rate of ammonia synthesis is shown and discussed. The atomic nitrogen flux to the rhodium crystal was calculated and a surface model presented.

## Rate Mechanism

Upon close observation, it can be seen that Figures 15 and 16 can be joined into one graph with no loss of information since there is no direct dependence on the hydrogen flow rate. The only dependence is on the atomic nitrogen pressure. The combined data are shown in Figure 17. A mechanism was formulated to model these results. This is shown in Figure 18. Using the steady state approximation for the coverage of atomic nitrogen on the surface, the following expression was derived:

$$N_S(d\Theta/dt) = 0 = k_1P_N(1-\Theta) - k_2\Theta - k_3\Theta^2 \qquad (4)$$

where $\Theta$ is the fraction of these sites occupied by atomic nitrogen and $N_S$ is the number of catalyst sites/cm$^2$ which can adsorb atomic nitrogen. The left side of Equation (4) represents the change in number of nitrogen adatoms/cm$^2$sec. The first term, $k_1P_N(1-\Theta)$, models the situation where the atomic N coverage for the surface is directly proportional to the atomic nitrogen pressure and adsorbs only on vacant sites. The second term, $k_2\Theta$, is for ammonia formation. Its only dependence is on the atomic nitrogen coverage. The hydrogen dependence can be assumed to be zero, because atomic hydrogen from the dissociation of molecular hydrogen is present in higher

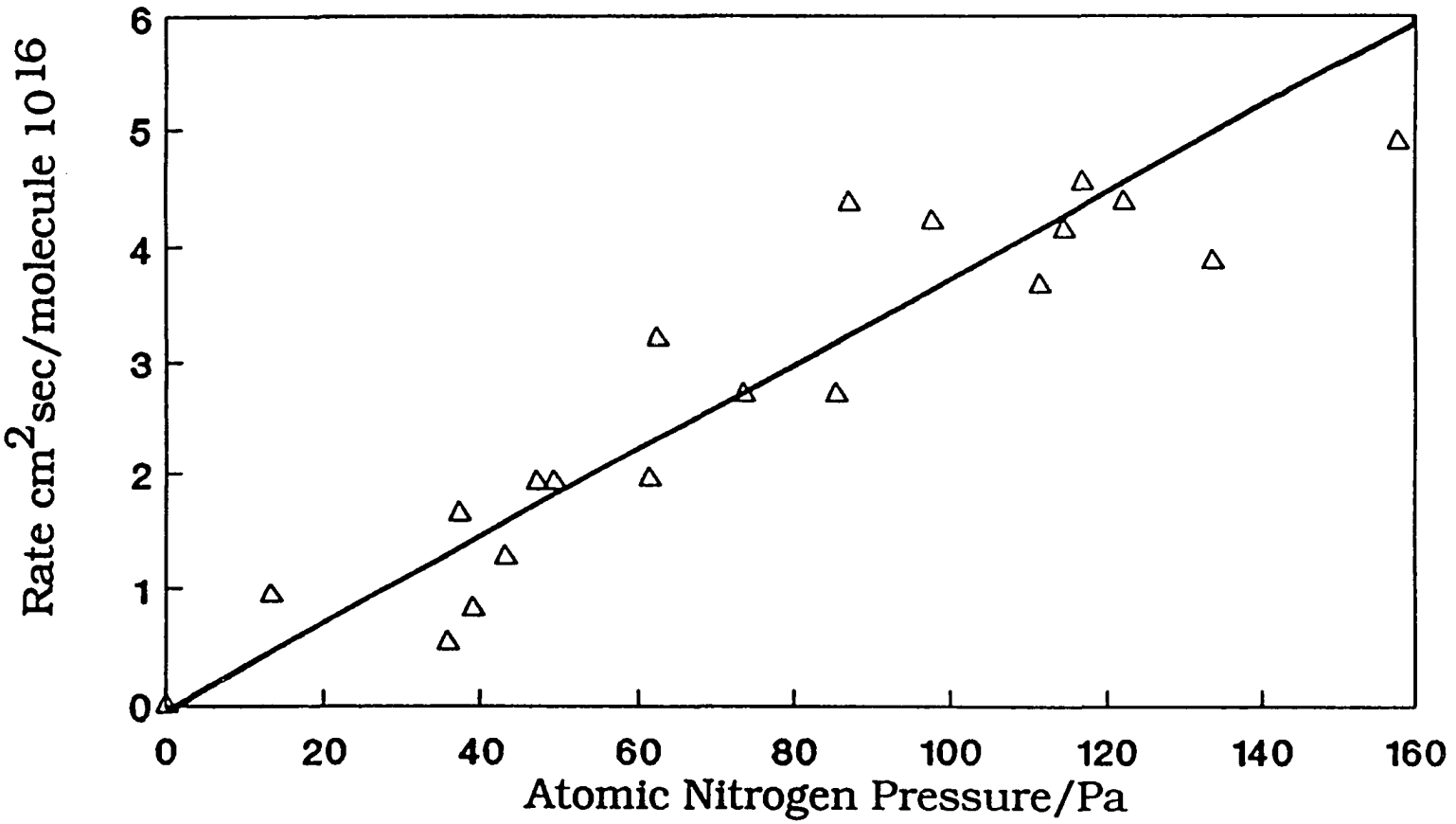


Figure 17. Dependence of the rate of ammonia production on atomic nitrogen pressure for a Rh(110) catalyst

Rate Mechanism

$k_1$ $N(g) \rightarrow N(ads)$

$H_2(g) \rightleftarrows H_2(ads)$

$H_2(ads) \rightleftarrows 2H(ads)$

$k_3$ $N(ads) + N(ads) \rightarrow N_2(ads)$

$N_2(ads) \rightarrow N_2(g)$

$k_2$ $N(ads) + H(ads) \rightarrow NH(ads)$

$NH(ads) + H(ads) \rightleftarrows NH_2(ads)$

$NH_2(ads) + H(ads) \rightleftarrows NH_3(ads)$

$NH_3(ads) \rightleftarrows NH_3(g)$

$$0 = (d\Theta/dt)N_S = k_1P_N(1-\Theta) - k_2\Theta - k_3\Theta^2$$

where

$\Theta$ = surface coverage of atomic nitrogen

Figure 18. The proposed rate mechanism shown in stepwise fashion for a Rh(110) catalyst

coverages for all the coverages of hydrogen and atomic nitrogen used. The third term, $k_3\Theta^2$, stands for the recombination of atomic nitrogen on the surface. In the gas phase this is a three body process; however the surface fulfills the role of the third body, absorbing the energy produced in the recombination.

This steady state equation has been solved for $\Theta$ to give

$$\Theta=[k_1P_Nf(x)]/(k_2 + k_1P_N) \qquad (5)$$

where $x = (4k_1P_N/k_3)\,[k_3/(k_1P_N + k_2)]^2$ and $f(x) = 2[(1 + x)^{0.5} - 1]/x$. Solving for the rate of ammonia formation, $k_2\Theta$, and the substitution for $\Theta$ gives

$$\text{Rate} = k_2\Theta N_S = k_2k_1P_Nf(x)/(k_1P_N + k_2). \qquad (6)$$

Properties of f(x) include $0 \le f(x) \le 1$ for $x>0$, $f(0) = 1$, and $f(x) \sim 2/x^{0.5}$ as $x \to \infty$. A plot of rate versus atomic nitrogen pressure is shown in Figure 19. The actual data points are represented by filled circles and the line is the best fit. If $x \ll 1$ and $f(x) \approx 1$, an approximation for $k_1$ and $k_2$ can be obtained by plotting $P_N$/Rate versus $P_N$. The resulting slope is the reciprocal of $k_2$ and the intercept is the reciprocal of $k_1$. The final values were elucidated by small variations in these rate constants and various constant values of $k_3$. The fitting was done with the assistance of a spreadsheet program, Wingz (Informix) which has simultaneous calculation and display of the results in graphical form. Values for the rate constants are as follows: $k_1 = 8.20 \times 10^{14}$ molecules $cm^{-2}$ $sec^{-1}$ $Pa^{-1}$, $k_2 = 7.62 \times 10^{16}$ molecules $cm^{-2}sec^{-1}$, and $k_3 = 1 \times 10^{16}$ molecules $cm^{-2}sec^{-1}$. With these parameters, Equation (5) with $P_N$=73.6 Pa leads to $\Theta = 0.44$. The rate of atomic nitrogen adsorption is $3.4 \times 10^{16}$ molecules/$cm^2$ sec, the rate of ammonia formation $3.2 \times 10^{16}$ molecules/$cm^2$ sec, and atomic nitrogen

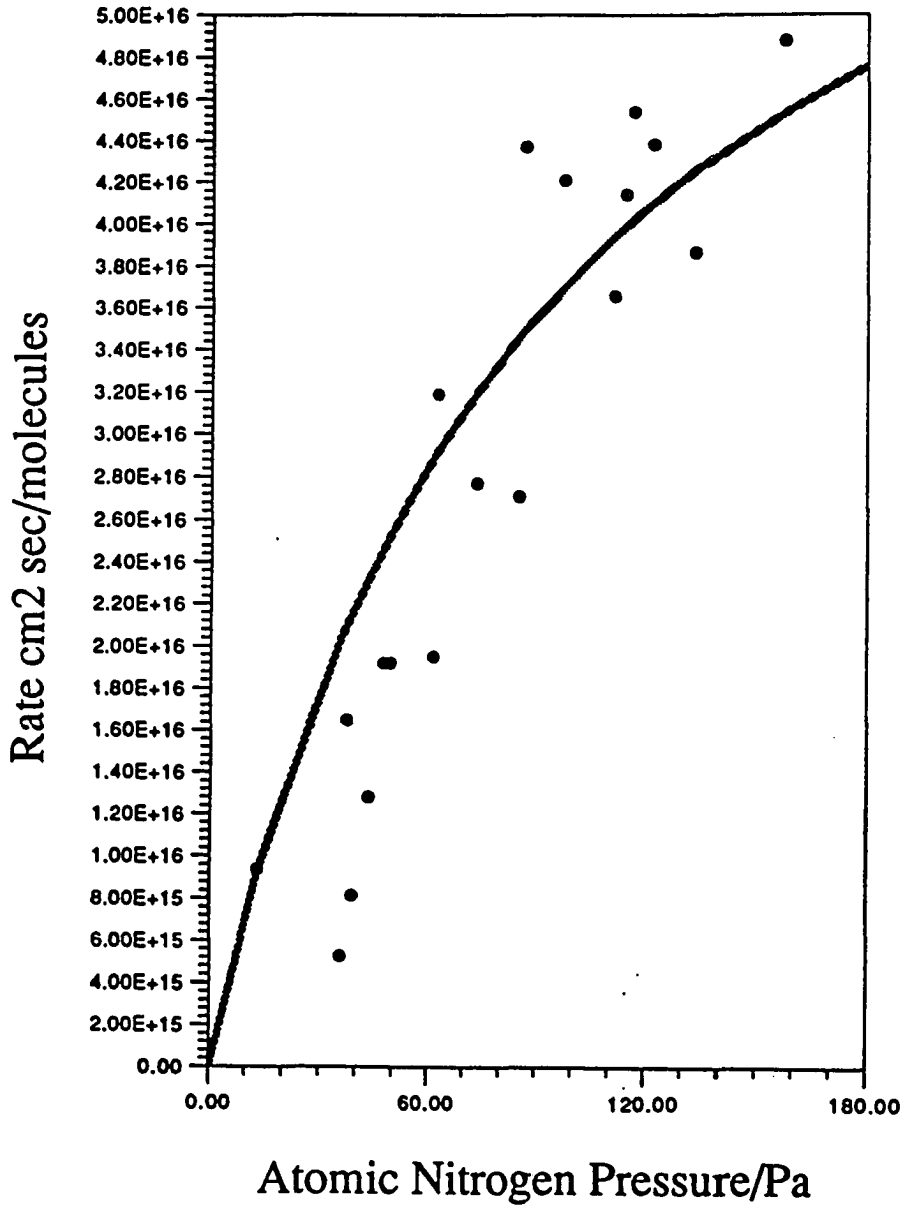


Figure 19. Dependence of the rate of ammonia production on atomic nitrogen pressure for a Rh(110) catalyst. The line corresponds to the rate mechanism shown in the text

adatoms are lost from the surface at a rate of $2 \times 10^{15}$ molecules/cm$^2$ sec. So the rate of atomic nitrogen adsorption is larger than the rate of ammonia formation with a small loss of ammonia production due to atomic nitrogen recombination on the surface.

**Arrhenius Plot**

Another point of interest is the activation energy of the reaction. The best route to this information is an Arrhenius plot of ln Rate versus 1/Temperature (K). Experimentally, the temperature was varied between 670 and 1020 K. The nitrogen flow rate was held constant at 1.3 ml/minute (160 Pa) and the hydrogen flow rate at 2.3 ml/minute (360 Pa). The results are shown in Figure 20. An apparent activation energy of -13 kJ/mole was observed and the pre-exponential factor was $3.0 \times 10^{15}$ molecules/cm$^2$sec. This same qualitative behavior was seen in the pH measurements to confirm the quantity of ammonia produced. As the temperature was lowered, the amount of ammonia produced increased in this range. An Fe catalyst at a total pressure of 1300 Pa (nitrogen and hydrogen) with a direct current plasma at 8 ma also exhibits the same behavior between 550 and 700 K, the rate of ammonia formation decreasing with temperature.[52] A negative apparent activation energy has also been observed for the oxidation of CO on Pd(111) at temperatures above 550 K.[53] This apparent negative activation energy can be explained in three possible ways, all of which involve processes which are favored by higher temperatures. The first is ammonia decomposition. Work by Vavere and Hansen[21] on Rh(110) for ammonia decomposition has shown that the rate of nitrogen evolution increases from $2 \times 10^{14}$ to $1 \times 10^{15}$ for temperature increase from 641 to 730 K. The ammonia pressure was 3.2 Pa and the Rate ~ $(P_{NH_3})^{0.5}$. The ammonia pressure for this set of experiments is

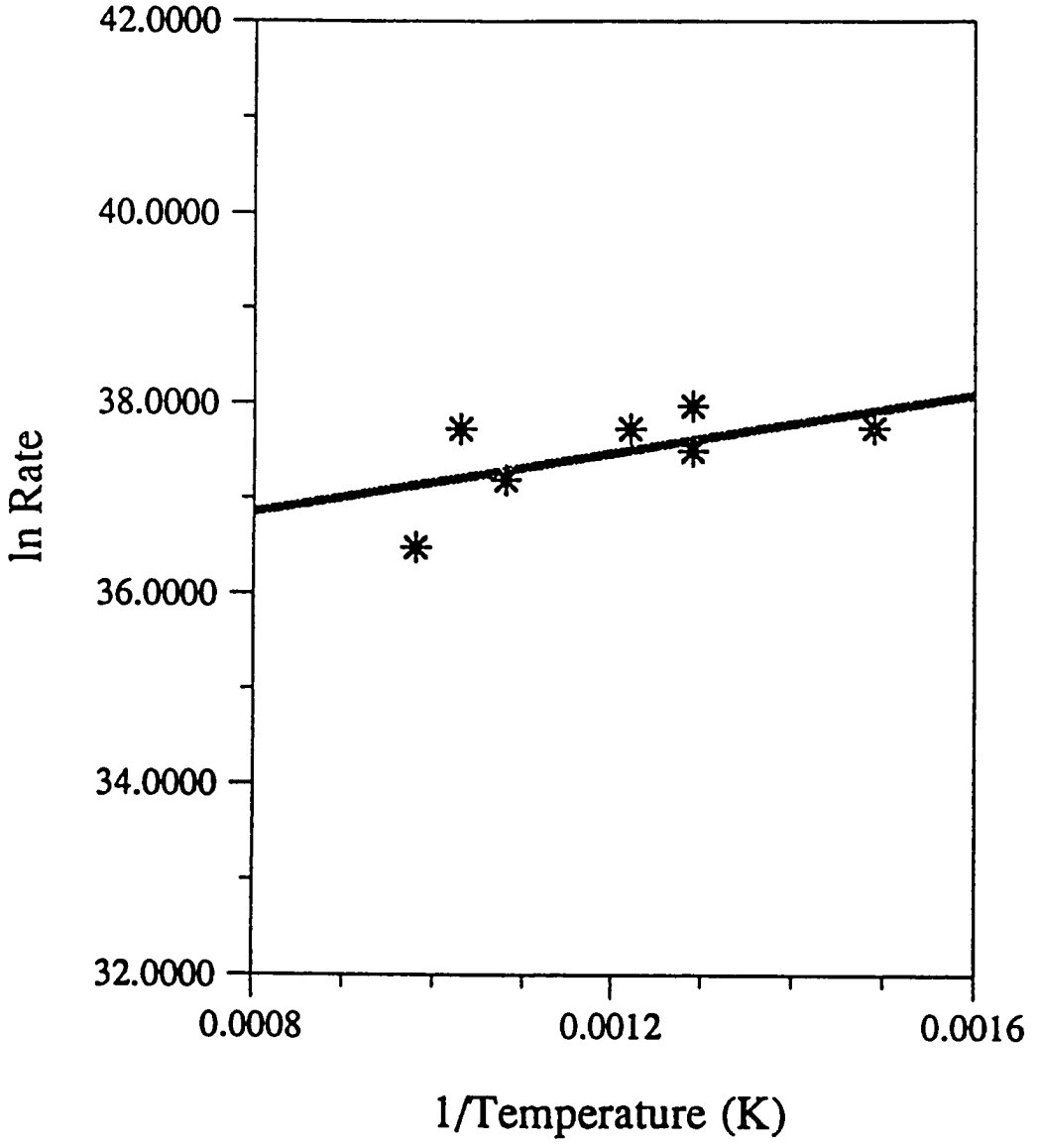


Figure 20. An Arrhenius plot showing the ln rate dependence on the inverse of the temperature at a constant nitrogen pressure of 160 Pa and a constant hydrogen pressure of 360 Pa for Rh(110)

estimated to be 16 Pa. Other results for ammonia decomposition on palladium at temperatures from 823 K to 973 K, at a ammonia pressure of 6,000 Pa, show a 36-fold increase in this range.[54] A second possibility is hydrogen deprivation at higher temperatures. Work by Mimeault and Hansen[55] and also by Yates, Thiel, and Weinberg[56] has shown that a substantial loss (a factor of six for temperatures between 700 and 1000 K) in hydrogen coverage results at higher temperatures. A third possibility is a larger rate of atomic nitrogen recombination at higher temperatures. An estimate using the calculated flux (described in the subsequent section) and results from the Hansen and Vavere paper[21] was too low to account for the observed rate variation. In conclusion, the ammonia decomposition argument is the most plausible of the three possibilities. The hydrogen deprivation causing the loss in rates at higher temperatures is also plausible, but the loss of hydrogen from this process would be offset by the hydrogen provided from ammonia decomposition.

### Atomic Nitrogen Flux

A question which should be addressed is: "What is the flux of atomic nitrogen to the crystal." As described earlier, the crystal was oriented perpendicular to the gas flow. A direct calculation would have been difficult, so instead we changed the crystal orientation and compared the rates of ammonia formation. A solution was found for the crystal oriented parallel to the gas flow and using equations in *Diffusional Mass Transfer*.[57] The flux to the crystal was determined in the following manner. The conditions were 5 torr total pressure (670 Pa) and a temperature of 450 C. (This temperature is an estimate of the gas temperature near the single crystal.) The atomic nitrogen concentration for this experiment was $1.2 \times 10^{-8}$ moles/cm$^3$. This was at

2.1 ml/minute nitrogen (220 Pa) and 2.8 ml/minute hydrogen flow rates (450 Pa). First an average mass transfer coefficient of 13.5 cm/sec was calculated using

$$k^*_{\rho m} = 0.646\,(D/L)(N_{Re})^{0.5}[\mu/\rho D]^{0.3} \qquad (10)$$

where L is the length of the single crystal, $\mu$ is the viscosity, D is the diffusion coefficient, $N_{Re}$ is the Reynolds number and $\rho$ is the density. The viscosity, diffusion coefficient, and Reynolds number were calculated using standard formulas. An average rate of mass transfer for the single crystal was then calculated:

$$q_{aw} = k^*_{\rho m}\,(\text{crystal area})(\text{atomic nitrogen concentration}) \quad (11)$$

This resulted in an average rate of mass transfer of $2.5 \times 10^{-7}$ moles atomic nitrogen/second. A total collection time of 2 hours was used for these experiments. The relative yield of ammonia for the perpendicular orientation compared to the parallel orientation is 1.67. It was assumed that an equal proportion of collisions of atomic N with the crystal were successful for both orientations and that any difference in the rate for the two orientations was due to changes in atomic N fluxes. The calculated amount of atomic N impacting the surface for the two hour experiment was $3 \times 10^{-3}$ moles N. Utilizing the rate constant for adsorption of atomic nitrogen from the gas phase determined earlier, a sticking coefficient $\approx 0.2$ was calculated for this particular set of flow rates. The ammonia yield under these conditions is $3.6 \times 10^{-4}$ moles which gives an ammonia yield from atomic nitrogen on the surface of 70 percent. Consequently atomic nitrogen recombination to form molecular nitrogen on the surface has a yield of 30% This compares with results by Halpern and Rosner, that the recombination of atomic nitrogen on polycrystalline rhodium wire proceeds with a 53% recom-

bination.[58]

An informative comparison can be made by comparing these results to those by Aika. Aika successfully synthesized ammonia at atmospheric pressure and 190° C using a Ru-K/C catalyst.[59] The rate calculated was 0.011 mmol $NH_3/day^{-1}$(g catalyst)$^{-1}$. This can be converted to 1.2 x $10^{12}$ molecules $cm^{-2}$ $sec^{-1}$ assuming a surface area of 2.2 $m^2/g$ catalyst for the 10 nm Ru particles. The rate for our experiments was 5 x $10^{16}$ molecules $cm^{-2}$ $sec^{-1}$.

## Surface Model

The first quantity of interest for the surface model is the surface coverage of atomic nitrogen. Using the kinetic model, estimates of $\Theta$ range from from 0.1 to 0.6 monolayers for atomic nitrogen gas pressures from 13 and 160 Pa. No direct analysis of the Rh(110) surface was done during these experiments. However, work by Kuwahara et al.[60] has investigated this system by EELS, Auger spectroscopy, and LEED. They have proposed a structure for Pd(110) which is structurally analogous to Rh(110) since both are face centered cubic metals with similar lattice constants (Rh 3.80 Å and Pd 3.89 Å). The atomic nitrogen was produced by electron impact dissociation of molecular nitrogen at 0.13 Pa nitrogen. The authors suggest on-top, short bridge, and long bridge sites for the atomic nitrogen. These sites are illustrated in Figure 21. B corresponds to the ontop site, A the short bridge, and C the long bridge site. I suspect that the long bridge site is most likely for low concentrations of atomic nitrogen because of the enhanced bonding provided by this site.

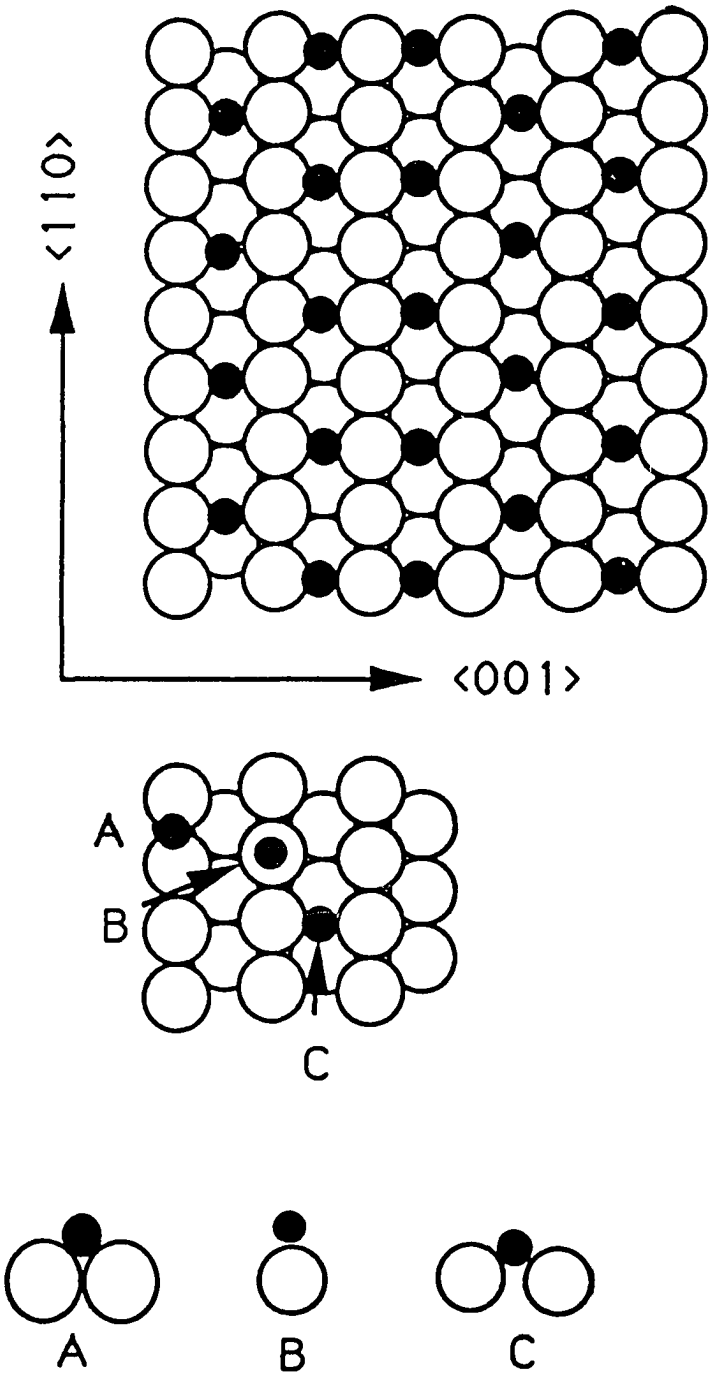


Figure 21. A model for the Rh(110) atomic nitrogen adsorption as proposed by Kuwahara et al. (60)

# SUMMARY

The synthesis of ammonia from hydrogen and atomic nitrogen on Rh(110) was studied using steady-state reaction kinetics. The atomic nitrogen was prepared by the use of a microwave plasma and quantified by a gas phase titration with nitric oxide. Under the following conditions which were 0.3 ml/minute < hydrogen flow rate < 10 ml/minute; 0.5 ml/minute < nitrogen flow rate < 8.3 ml/minute; 110 Pa < $P_{H_2}$ < 1000 Pa; 100 Pa < $P_{N_2}$ < 570 Pa; 13 Pa < $P_N$ < 160 Pa and a temperature of 500 C, the rate was found to depend only on the atomic nitrogen pressure. This is in accordance with earlier results for platinum gauze. Spectroscopic characterization of the afterglow provided no evidence of the formation of NH, $NH_2$, or $NH_3$ in the gas phase. Turnover numbers range from 0.0079 - 0.066 molecules site$^{-1}$ sec$^{-1}$ for nitrogen flow rates between 0.5 and 8.3 ml/minute which correspond to pressures between 100 and 570 Pa while the hydrogen flow rate was held constant at 2.8 ml/minute (450 Pa). The turnover numbers for hydrogen flow rates between 0.3 and 10 ml/minute (110-1000 Pa) for constant nitrogen flow rate of 2.1 ml/minute (220 Pa) are 0.014 - 0.073 molecules site$^{-1}$ sec$^{-1}$ . The atomic nitrogen pressure varied from 13 Pa to 160 Pa. The total pressure inside the system ranged from 330 Pa - 1200 Pa. A metal catalyst (platinum and rhodium have been demonstrated) is crucial to the success of the reaction. Under the conditions stated for the plasma, no ammonia is produced unless the catalyst is present.

The rate of production for ammonia synthesis reaches a maximum of 4.4 x $10^{16}$ molecules/cm$^2$ sec for a nitrogen flow rate of 5 ml/minute (430 Pa) and decreases slowly for higher nitrogen flow rates. The rate of production for ammonia synthesis increases proportionally with increasing hydrogen flow rates. The first

question is whether a species produced in the plasma was responsible for these results. These species include atomic nitrogen, A $^3\Sigma_u^+$ state of molecular nitrogen, atomic hydrogen hydrogen and various electronically excited states of molecular hydrogen. Spectroscopically, electronically excited states of molecular nitrogen and atomic hydrogen were seen. However, the presence of atomic nitrogen and electronically excited molecular hydrogen can be inferred from these data. The A state of nitrogen can be formed in two ways. The first way is from the plasma directly and the second is from the recombination of N atoms in the gas phase.

Atomic nitrogen is formed in a microwave plasma at 62 watts power. The atomic nitrogen pressure increases with nitrogen flow rates until 3.0 ml/minute (130 Pa) is reached and then decreases slowly for higher flow rates. To my initial surprise, the atomic nitrogen concentration also depends on hydrogen flow rates between 0.3 and 10 ml/minute (110-1000 Pa). The pressure of atomic nitrogen increases proportionally with increasing hydrogen flow rates for this range.

The rate of ammonia production is directly proportional to the atomic nitrogen pressure. There is no dependence on the hydrogen pressure for the rate of ammonia production for 110 Pa< $P_{H_2}$< 1000 Pa and 100 Pa< $P_{N_2}$< 570 Pa. The data were fit with a rate law with the following assumptions: (1) the rate of ammonia formation is proportional to the atomic nitrogen coverage on the surface, (2) the recombination of atomic nitrogen to form molecular nitrogen is dependent on the square of the atomic nitrogen coverage, (3) the rate of atomic nitrogen adsorption on the surface is dependent on the number of sites available and the pressure of atomic nitrogen in the gas phase. The apparent activation energy for ammonia production is -18 kJ/mole.

In conclusion, ammonia was synthesized catalytically on Rh(110) and

polycrystalline platinum at low pressures (~ 200 Pa) for nitrogen and hydrogen. The gases were "activated" via a microwave plasma before being flowed over the metal catalyst. No ammonia was produced in the absence of a catalyst. Analysis of the plasma afterglow showed a variety of excited nitrogen species including atomic nitrogen were present. By delaying access to the catalyst, excited nitrogen species other than atomic nitrogen were eliminated because of their short lifetimes. It was proved that the presence of atomic nitrogen is sufficient to lead to low pressure ammonia synthesis. Finally, a model based solely on atomic nitrogen pressure with its corresponding rates of adsorption, hydrogenation and recombination was shown to account for the ammonia synthesis rates observed.

# BIBLIOGRAPHY


1. *Chem. Eng. News* **1989**, *67*, 39.
2. *Catalyst Handbook*; Wolfe Scientific Books: London, 1970; Chapter 7.
3. *Catalyst Handbook*; Twigg, M.; Ed.; Wolfe Publishing Ltd: London, 1989; Chapter 8.
4. Grunze, M. In *Chemical Physics of Solid Surfaces and Heterogeneous Catalysis*; King, D. A.; Woodruff, D. P.; Eds.; Elsevier: New York, 1982; Vol. 4, Chapter 5.
5. Emmett, P. H. In *Physical Basis for Heterogeneous Catalysis*; Drauglis, E.; Jaffee, R. I.; Eds., Plenum Press: New York, 1975; Chapter 1.
6. Gordon, A. J. *The Chemist's Companion*; Wiley: New York, 1972; p 113.
7. I. R. Shannon In *Catalysis*; Kemball, C.; Dowden, D. A.; Senior Reporters; Specialist Periodical Report; The Chemical Society: London 1978; Vol. 2, Chapter 2.
8. Ozaki, A.; Aika, K. In *Catalysis*; Anderson, J. R.; Boudart, M.; Eds.; Springer Verlag: New York, 1981; Chapter 3.
9. Ozaki, A.; Aika, K. In *A Treatise on Dinitrogen Fixation*; Hardy, J.; Ed.; John Wiley & Sons: New York, 1979; Vol. 4, Chapter 4.

10. Scholten, J. J. F.; Zwietering, P. *Trans. Faraday Society* **1957**, *53*, 1363.
11. Ertl, G. *CRC Crit. Rev. Solid State Mater. Sci.* **1980**, *10*, 349.
12. Bozso, F.; Ertl, G.; Weiss, M. *J. Catal.* **1977**, *50*, 519.
13. Spencer, R. C.; Schonmaker, G. A.; Somorjai, G. *Nature* **1981**, *294*, 643.
14. Whitman, L. J.; Bartosch, C. E.; Ho, W. *J. Chem. Phys.* **1986**, *85*, 3688.
15. Bassignana, I. C.; Wagemann, K.; Kuers, J.; Ertl, G. *Surf. Sci.* **1986**, *175*, 22.
16. Obuchi, A.; Naito, S.; Onishi, T.; Tamaru, K. *Surf. Sci.* **1983**, *130*, 29.
17. Wilf, M.; Dawson, P. T. *Surf. Sci.* **1976**, *60*, 561.
18. Horn,K.; DiNardo, J.; Eberhardt, W.; Freund, H.-J.; Plummer, E. W. *Surf. Sci.* **1982**, *118*, 465.
19. Ibbotson, D. E.; Wittrig, T. S.; Weinberg, W. H.; *Surf. Sci.* **1981**, *110*, 313.
20. Aika, K.; Yamaguchi, J.; Ozaki, A. *Chem. Lett.* **1973**, 161.
21. Hansen, R. S.; Vavere, A. *J. Catal.* **1981**, *69*, 158.
22. Campbell, C. T.; White, J. M. *Appl. Surf. Sci.* **1978**, *1*,347

23. Grunze, M.; Golze, M.; Hirschwald, W.; Freund, H.-J.; Pulm, H.; Seip, U.; Tsai, M.-C.; Ertl, G.; Kuppers, J. *Phys. Rev. Lett.* **1984**, *53*, 850.

24. Tsai, M. C.; Seip, U.; Bassignana, I. C.; Kuppers, J.; Ertl, G. *Surf. Sci.* **1985**, *155*, 387.

25. Freund, H.-J.; Bartos, B.; Messmer, R. P. *Surf. Sci.* **1987**, *185*, 187.

26. Matsushita, K. I.; Hansen, R. S. *J. Chem. Phys.* **1970**, *52*, 3619.

27. Brown, R.; Winkler, C. A. *Angew. Chem, Internat. Ed.* **1970**, *9*, 181.

28. Clyne, Michael A. A.; Wing, S. In *Reactive Intermediates in the Gas Phase*; Setser, D. W.; Ed.; Academic Press: New York, 1979; Chapter 1.

29. Foner, S. N.; Hudson, R. L. *J. Chem. Phys.* **1962**, *37*, 1662.

30. Vidaud, P. H.; Wayne, R. P.; Yaron, M.; von Engel, A. *J. Chem. Soc. Farad. Trans. 2* **1976**, *72*, 1185.

31. Botchway, G. Y.; Venugopalan, M. *Z. fur Phys. Chem. NF* **1980**, *120*, 103.

32. Eremin, E. N.; Mal'tsev, A. N.; Belova, V. M. *Russ. J. Phys. Chem. (Engl. Transl.)* **1971**,*45*, 205.

33. Eremin, E. N.; Mal'tsev, A. N.; Syaduk, V. L. *Russ J. Phys. Chem.(Engl. Transl.)* **1971**, *45*, 635.

34. Uyama, H.; Matsumoto, O. *Plasma Chem. Plasma Process.* **1989**, *9*, 13.

35. Uyama, H.; Matsumoto, O. *Plasma Chem. Plasma Process.* **1989**, *9*, 271.

36. Mantell, D. A.; Kunimori, K.; Ryali, S. B.; Haller, G. L. Fenn, J. B. *Surf. Sci.* **1986**, *172*, 281.

37. Foner, S. N.; Hudson, R. L. *J. Chem. Phys.* **1984**, *80*, 518.

38. Zander, A. T.; Hieftje, G. M. *Appl. Spec.* **1981**, *35*. 357.

39. McCarroll, B. *Rev. Sci. Instrum.* **1970**, *41*, 279.

40. Fehsenfeld, F. C.; Evenson, K. M.; Broida, H. P. *Rev. Sci. Instrum.* **1965**, *36*, 294.

41. McTaggart, F. K. *Plasma Chemistry in Electrical Discharges*; Elsevier: New York, 1967; Chapter 2.

42. Brocklehurst, B.; Jennings, K. R. In *Progress in Reaction Kinetics*; Porter, G.; Ed.; Pergamon Press: Oxford, 1967; Vol. 4, Chapter 1.

43. Harteck, P.; Reeves, R. R.; Mannella, G. *J. Chem. Phys.***1954**, *29*, 608.

44. Clyne, M. A. A.; McDermid, I. S. *J. Chem. Soc. Faraday Trans. 1*, **1975**, *71*, 2189.

45. Kaufman, F. In *Progress in Reaction Kinetics*; Porter, G.; Ed.; Academic Press: New York, 1961; Vol. 1, Chapter 1.

46. Pearse, R. W. B.; Gaydon, A. G. *The Identification of Molecular Spectra*; John Wiley & Sons: New York, 1976; pp 235-242.

47. Meyer, J. A.; Setser, D. W.; Stedman, D. H. *J. Phys. Chem.* **1970**, *74*, 2238.

48. Kolts, J. H.; Setser, D. W. In *Reactive Intermediates in the Gas Phase* Setser, D. W.; Ed.; Academic Press: New York, 1979; Chapter 3.

49. Lin, M. C.; McDonald, J. R. In *Reactive Intermediates in the Gas Phase* Setser, D. W.; Ed.; Academic Press: New York, 1979; Chapter 4.

50. Clyne, M. A. A.; Stedman, D. H. *J. Phys. Chem.* **1967**, *71*, 3071.

51. Giridhar, R. V.; Rose, K. *Mater. Res. Soc. Symp. Proc.* **1985**, *38*, 451.

52. Veprek, S.; Venugopalan, M. In *Topics in Current Chemistry*; Boschke, F. L.; Ed.; Springer-Verlag: New York, 1983; Vol. 107, p 29.

53. Engel, T; Ertl, G.; *J. Chem. Phys.* **1978**, *69*, 1267.

54. Mardaleishvili, R. E., Hsing-Chou, H., Smorodinskaya, Zh.Ya. *Kinet. Katal.* **1969**, *10*, 1278.

55. Mimeault,V.J.; Hansen, R.S.*J. Chem. Phys.***1966**,*45*, 2240.

56. Yates, J.T.; Thiel, P.A., Weinberg, W.H. *Surf. Sci.* **1979**, *84*, 427.

57. Skelland, A. H. P. *Diffusional Mass Transfer*, John Wiley and Sons: New York, 1974; p 119.

58. Halpern, B.; Rosner, D. *J. Chem. Soc. Faraday Trans. 1* **1978**, *74*, 1883.

59. Aika, K. *Angew. Chem. Int. Ed. Engl.* **1986**, *25*, 558.

60. Kuwahara, Y.; Fujisawa, M.; Jo, M.; Onchi, M.; Nishijima, M. *Surf. Sci.* **1987**, *188*, 490.

61. Rainwater, J.C.; Biolsi, L.; Biolsi, K.; Holland, P.M. *J. Chem. Phys.***1983**, *79*, 1462.

# ACKNOWLEDGMENTS

The author wishes to thank Professor Hansen for his encouragement, support, enthusiasm and numerous comments on this project. She especially appreciates his flexibility and patience. In addition, the author wishes to thank Ames Laboratory, DOE, for support and equipment. She would also like to thank the machine shop and glass shop for all of their assistance. Thanks are also due to Professor Thiel for the use of her crystal mounting tools and other specialized equipment. Dr. K.G. Baikerikar is fondly remembered as an excellent person to share one's space. Jim Anderegg's touch with mechanical difficulties was much appreciated.

Special thanks are due to my husband for sharing his desk. Even more, his encouragement and support has been invaluable.

# APPENDIX I: SPECTROSCOPIC ANALYSIS OF AFTERGLOW

Figure 3.

1.6 ml/minute Nitrogen

| Wavelength (nm) | Identity of Peak |
|---|---|
| 297 | Oxygen atoms |
| 314 | Nitrogen 2nd Positive |
| 337 | Nitrogen 2nd Positive |
| 354 | Nitrogen 2nd Positive |
| 371 | Nitrogen 2nd Positive |
| 376 | Nitrogen 2nd Positive |
| 380 | Nitrogen 2nd Positive |
| 590 | Sodium |
| 654 | Nitrogen 1st Positive |
| 739 | Nitrogen 1st Positive |
| 750 | Nitrogen 1st Positive |
| 763 | Nitrogen 1st Positive |

Figure 4.

4.5 ml/minute Hydrogen

| Wavelength (nm) | Identity of Peak |
|---|---|
| 486 | Atomic Hydrogen |
| 589 | Sodium |
| 656 | Atomic Hydrogen |

Figure 5.

1.6 ml/minute Nitrogen and 1.3 ml/minute Hydrogen

| Wavelength (nm) | Identity of Peak | Vibrational State (v',v") |
|---|---|---|
| 297 | Oxygen atoms | |
| 314 | Nitrogen 2nd Positive | 2,1 |
| 337 | Nitrogen 2nd Positive | 0,0 |
| 354 | Nitrogen 2nd Positive | 1,2 |
| 358 | Nitrogen 2nd Positive | 0,1 |
| 376 | Nitrogen 2nd Positive | 1,3 |
| 380 | Nitrogen 2nd Positive | 0,2 |
| 400 | Nitrogen 2nd Positive | 0,4 |
| 486 | Atomic Hydrogen | |
| 590 | Sodium | |
| 656 | Atomic Hydrogen | |

Figure 6.

1.6 ml/minute Nitrogen and 4.5 ml/minute Hydrogen

| Wavelength (nm) | Identity of Peak | Vibrational State (v',v") |
|---|---|---|
| 297 | Oxygen atoms | |
| 314 | Nitrogen 2nd Positive | 2,1 |
| 337 | Nitrogen 2nd Positive | 0,0 |
| 354 | Nitrogen 2nd Positive | 1,2 |
| 358 | Nitrogen 2nd Positive | 0,1 |
| 371 | Nitrogen 2nd Positive | 2,4 |
| 380 | Nitrogen 2nd Positive | 0,2 |
| 390 | Nitrogen 2nd Positive | 3,6 |
| 394 | Nitrogen 2nd Positive | 2,5 |
| 400 | Nitrogen 2nd Positive | 0,4 |
| 414 | Nitrogen 2nd Positive | 3,7 |
| 420 | Nitrogen 2nd Positive | 2,6 |
| 427 | Nitrogen 2nd Positive | 1,5 |
| 486 | Atomic Hydrogen | |
| 590 | Sodium | |
| 656 | Atomic Hydrogen | |

# APPENDIX II: FLUX CALCULATIONS

According to the kinetic theory of gases, the transport properties such as viscosity and diffusion coefficients depend on the two-body interactions between chemical species. When two ground state ($^4S$) nitrogen atoms interact, they can follow any of four potential energy curves (states) corresponding to the nitrogen molecule; the ground state $X^1\Sigma_g^+$ and the $A\ ^3\Sigma_u^+$, $^5\Sigma_g^+$, and $^7\Sigma_u^+$ states.[61] The following values were substituted in the formulas displayed below: M=14, p = 6.70 x $10^{-3}$ in units of 0.1 MPa (1 bar), T = 450 K, $\sigma^2\Omega^{(2,2)*}$ = 7.241 in units of $10^{-20}$ $m^2$ at 1000 K, and $\sigma^2\Omega^{(1,1)*}$ = 6.4576 in units of $10^{-20}$ $m^2$ at 1000 K. The nearest tabulated values for the integrals were for temperatures of 1000 K.

$$\mu = 2.669 \times 10^{-5} \frac{\sqrt{MT}}{\sigma^2\Omega^{(2,2)*}}$$

$$\mu = 2.92 \times 10^{-4} \text{ poise}$$

$$D = \frac{2.694 \times 10^{-3} \sqrt{T^3/M}}{p\sigma^2\Omega^{(1,1)*}} \text{ cm}^2/\text{sec} = 230 \text{ cm}^2/\text{sec}$$

$$N_{Re} = \frac{\rho v L}{\mu} = \frac{(1.7 \times 10^{-7} \text{ g/cm}^3)(3.8 \text{ cm/sec})(0.9 \text{ cm})}{2.92 \times 10^{-4} \text{ poise}}$$

$$= 2.0 \times 10^{-3}$$

$$k^*_{\rho m} = 0.646 \frac{D}{L} \sqrt{N_{Re}} \left[\frac{\mu}{\rho D}\right]^{0.3}$$

$$= (0.646)(230 \text{ cm}^2/\text{sec})(1/0.9 \text{ cm})(2.0 \times 10^{-3})^{0.5} \left[\frac{2.92 \times 10^{-4} \text{g/cm sec}}{(1.7 \times 10^{-7})(230 \text{ cm}^2/\text{sec})}\right]^{0.3}$$

$$= 13.5 \text{ cm/sec}$$

$q_{aw} = k^* \rho_m$ (crystal area)(atomic nitrogen concentration)

$= (13.5 \text{ cm/sec})(1.55 \text{ cm}^2)(1.2 \times 10^{-8} \text{ moles/cm}^3)$

$= 2.5 \times 10^{-7}$ moles atomic N/sec at the surface

All of the preceding calculations are for the parallel orientation. Using the experimentally derived factor of 1.67 for the enhanced collision rate due to the perpendicular orientation, results in an adjusted $q_{aw}$ of $4.2 \times 10^{-7}$moles atomic N/sec. For these two hour experiments, the total amount of atomic nitrogen colliding with the surface is $3 \times 10^{-3}$ moles.

Using the kinetic model presented for the rate of ammonia synthesis allows to calculate the rate of atomic nitrogen adsorption on the surface. For this case of 220 Pa molecular nitrogen and 450 Pa hydrogen, the atomic nitrogen pressure is 47 Pa and the rate of ammonia formation is $1.9 \times 10^{16}$ molecules/cm$^2$sec.

$(\text{Rate})_{\text{ammonia formation}} = k_2\Theta$

Utilizing the value for $k_2$ obtained earlier, an estimate of $\Theta = 0.25$ results. Also from the earlier section, the

$(\text{Rate})_{\text{atomic nitrogen adsorption}} = k_1 P_N(1-\Theta)$

This rate equals $2.9 \times 10^{16}$ atoms/cm$^2$ sec for this case. The total atomic nitrogen adsorbed can be calculated as follows:

$(\text{Rate})_{\text{atomic nitrogen adsorption}}$ (crystal area)(7200 sec)/$6.022 \times 10^{23}$

A total of $5 \times 10^{-4}$ moles of atomic nitrogen was adsorbed in the course of this particular experiment. A sticking coefficient of approximately 0.2 can be estimated by dividing the moles of nitrogen adsorbed by the moles of nitrogen which collided with the surface.